Charge-Based Noise Analysis for Distal Synapses

Michael T. Smith

Master of Science
School of Informatics
University of Edinburgh
2008

Abstract

Various synaptic properties can be quantified by analysing the flow of synaptic current. For example, by examining the variance in the current between different impulse responses, the size and number of ion channels can be deduced. If a synapse is distal, the current can become distorted as it travels through the dendrite. The distortion has a severe effect on the parameter estimates, which become invalid even for a relatively nearby synapse.

This thesis develops and applies an alternative technique, which uses the variance in the total charge instead of current. The technique is shown to work for a local synapse using a model of an AMPA synapse. It is then applied to a distal synapse, and the distortion in the estimate compared to that from the current-based analysis. The distortion is corrected for, using assumptions about the cable filtering. The result is a theoretical method for estimating channel parameters in distal synapses.

Acknowledgements

Many thanks to my supervisor, Mark van Rossum, for his help and support. I also would like to acknowledge Adam Barrett, who developed the charge and variance solutions used in Chapter 3 and Rob Smith for his help with the NeuronC simulator.

Declaration

I declare that this thesis was composed by myself, that the work contained herein is my own except where explicitly stated otherwise in the text, and that this work has not been submitted for any other degree or professional qualification except as specified.

(*Michael T. Smith*)

To Lyndsey, Lilly and Lolly

Table of Contents

Chapter 1

Introduction

1.1 Background

1.1.1 Discovery of Ion channels and their Properties

In 1783, Luigi Galvani performed several experiments with ‘animal electricity’. He showed that an electric current could be used to control muscles, and that this current travelled through nerves[3]. Since then researchers have attempted to understand how nerves transmit and store information. At the end of the 19th century, Sir Charles S. Sherrington developed the concept of the synapse. This could explain why current flowed across the junction in only one direction and how inhibitory junctions were possible[13].

In 1952, Alan Hodgkin and Andrew Huxley discovered that small changes in a nerve’s membrane potential caused large changes in ionic current. From this they deduced that the potassium and sodium ions must pass through ‘active patches’ or channels. The current caused by the movement of the charged particles within the membrane was undetectable[5], which meant that there were relatively few of these patches. They also suggested that the potassium and sodium ions passed through different patches. In 1964, Toshio Narahashi, John W. Moore and William R. Scott proved this hypothesis by blocking sodium ion channels selectively using Tetrodotoxin[11].

1.1.2 Synaptic Noise

During the ’60s there was much debate about the cause of fluctuations and noise in the synaptic current. In 1972 Charles Stevens published a paper[21] explaining how this noise could be analysed to find the single channel conductance. He predicted that this conductance would be equal to the ratio between the mean and the variance of the total synaptic conductance (in the limit of low neurotransmitter concentration). This was followed by many papers which used the technique described. For example, Fred Sigworth in 1980 applied it to sodium current at

the Node of Ranvier[18]. In 1975, van der Berg et al. used the fluctuations to estimate the single channel conductance, using a different technique[23].

Detailed recordings of single ion channels became possible with the invention of the patch clamp in 1976, which could isolate a small patch of membrane[4]. The technique was refined and is now used by thousands of researchers every year[1].

Although the behaviour of many channel types can now be recorded directly using the patch clamp technique, some, such as those at an intact post-synaptic site remain inaccessible. The pre-synaptic membrane covers the synapse and the small size of the post-synaptic density makes patch clamping just one synapse currently very difficult[17]. Although patch clamps have been successfully applied to dendrites with diameters of less than 2 μm [22], recording an intact, functioning synapse is only just becoming possible using this technique.

1.1.3 Current-based Fluctuation Analysis

Understanding synaptic plasticity, and the effect of different agonists, requires intact synapses during the experiment. For instance, attempting to record the changes in the synapse due to long term potentiation requires the synapse to remain functioning and attached to the presynaptic axon terminal. Fluctuation analysis doesn't damage the synapse, allowing these recordings to be made.

Fluctuation analysis relies on how the variance in the current flow and the channel open probability are related. Consider just one channel for the moment. It is open with probability p and, if open, allows a current i_0 to flow. The mean current, over many trials is written $\langle i \rangle$, and is equal to pi_0. The mean squared current, $\langle i^2 \rangle$, is pi_0^2.

The variance of a random variable, x, is defined to be:

$$\sigma_x^2 = \langle x^2 \rangle - \langle x \rangle^2 \tag{1.1}$$

So the variance of the current, i, sampled over many trials, will be:

$$\sigma_i^2 = pi_0^2 - (pi_0)^2 = p(1-p)i_0^2 \tag{1.2}$$

The mean and variance of the sum of N independent distributions will be the sum of their means and variances. So to calculate the variance in the total mean current, I, from N channels we simply multiply the mean and variance by N. The mean then becomes:

$$I = Npi_0 \tag{1.3}$$

And the variance:

$$\sigma_I^2 = N\left(pi_0^2 - (pi_0)^2\right) = Npi_0^2 - Np^2i_0^2 \tag{1.4}$$

Using equation 1.3, equation 1.4 can be rewritten:

$$\sigma_I^2 = i_0\left(Npi_0 - Np^2i_0\right) = i_0\left(I - Ip\right) = i_0I(1-p) \tag{1.5}$$

This variance is the same as that for a binomial distribution, and so forms a parabola as p varies from 0 to 1. This can be understood intuitively by considering the variance for different values of p. With $p = 0$, the variance will be zero, as all the channels will be shut. With $p = 1$, all the channels are open, and there will be no variance between trials in the number of open channels. The binomial distribution's variance peaks when $p = 0.5$, this will cause the most variation between trials. To find the single channel current, rearrange equation 1.5 for i_0:

$$i_0 = \frac{\sigma_I^2}{I(1-p)} \tag{1.6}$$

If the probability of opening is small, then this can be simplified to:

$$i_0 \rightarrow \frac{\sigma_I^2}{I} \ \ as \ \ p \rightarrow 0 \tag{1.7}$$

If the variance, σ_I^2, is plotted against the mean current I, then, as mentioned above, the curve drawn is parabolic. As $p \rightarrow 0$, the variance and mean current approach zero. Also the ratio of the variance and the mean, as stated in equation 1.7 approach the single channel conductance, i_0. This ratio is approximately the initial gradient of the parabola. So the initial gradient of the parabola approximately equals the single channel current.

Two forms of analysis exist to measure these membrane parameters. Stationary and Non-stationary analysis. Stationary analysis requires the experimenter to record the steady-state current and variance for different open probabilities. These can be plotted against each other and the gradient of the line formed will allow i_0 to be estimated.

There are several problems with this technique. The first is the assumption of low open probability. In many cases this would be unsound. Second, it gives no indication of the number of channels. Third, other sources of noise will add to the apparent variance, biasing the result.

Sigworth's non-stationary analysis[18] avoids these problems by measuring the current during the application of a voltage step. The same step is applied many times, and the variance and mean at each time step between the different recordings can be calculated. The mean and variance are plotted against each other and form a parabola, as described above. Figure 1.1 is from Sigworth's 1980 paper and illustrates such a curve.

The number of ion channels can also be estimated using the parabola. The point at which all the channels are open will have zero variance. At this point the curve meets the x-axis again and the mean current indicates the current that would flow if all the channels were open. Dividing this value by the single channel current gives the number of channels.

Note that if there is noise in the signal, besides that caused by the channels opening and closing, the parabola will not intersect the origin, but will start with some variance. This extra variance can be assumed to be caused by noise uncorrelated with the open probability, p, and can therefore be subtracted, leaving the parabola intersecting the origin as before.

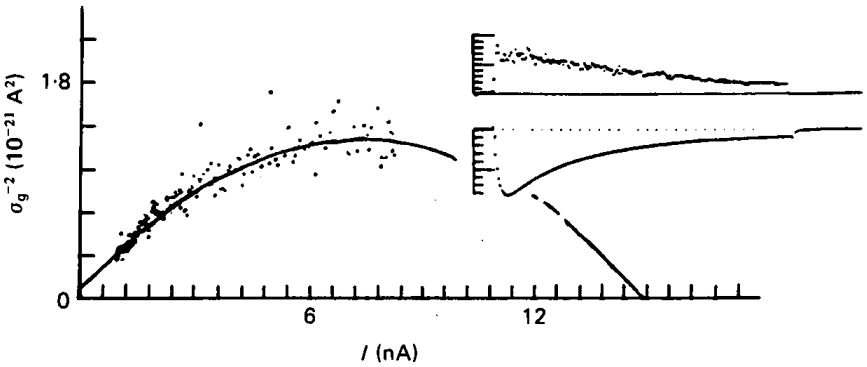

Figure 1.1: *Example of a current-variance plot, taken from Sigworth's 1980 paper [18]. The insets show the time course of the variance (top) and mean current (bottom). When plotted against each other (main plot), a parabola is formed.*

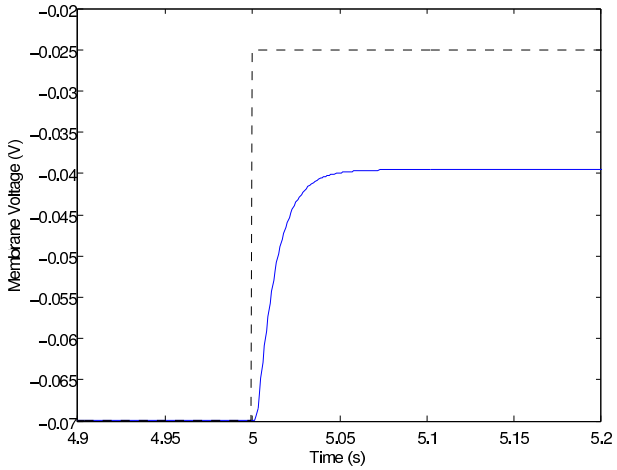

Figure 1.2: *Effect of cable filtering. A voltage clamp is applied after 5s to one end of the dendrite. The black dashed line indicates the membrane voltage at this point. 700 µm from this point the voltage is also recorded (blue solid line), which is approximately one space constant from the clamp.*

1.2 Problems with Current Fluctuation Analysis

1.2.1 Cable Filtering

In most cases, the synapse being recorded is a long way from the recording microelectrode. For instance, a synapse, on the dendrite, may be far from the Soma where the microelectrode is usually inserted. The long length of dendrite between the two distorts the signal, causing the fluctuation analysis to underestimate the single channel current. Figure 1.2 illustrates the effect of cable filtering over a short stretch of dendrite and figure 1.3 illustrates how the estimate of the single channel current is affected by the cable filtering. Clearly the current-based analysis will not work for distal synapses.

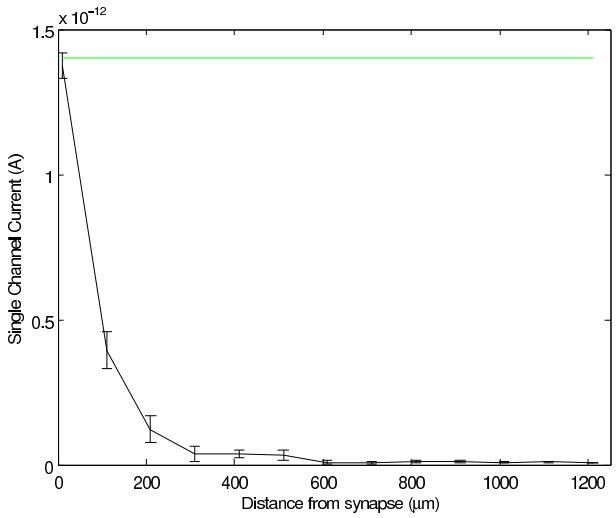

Figure 1.3: *Later in this thesis the effect of cable filtering will be examined more closely. This figure, based on an example from chapter 7, illustrates the effect of cable filtering on the estimate of the single channel current. The green line indicates the actual single channel current, while the black line indicates the estimated value, using the current based fluctuation analysis applied to recordings from the soma. The signal becomes more distorted the further the synapse is from the soma, causing the parabola to change shape, and thus cause the change in the estimate of the channel current.*

1.2.2 Excitatory and Inhibitory Receptors

If the same types of receptor were found to be distributed evenly across the whole of the cell, then only being able to record at the soma may not be a problem. However, it's been found that the proportion, type and size of inhibitory and excitatory synapses vary depending on the type of dendrite and its distance from the Soma[10]. For instance excitatory AMPA receptors have been found in much higher concentrations on distal narrow dendrites than on proximal thick dendrites.

1.2.3 Charge instead of Current

To avoid the more severe forms of cable filtering, this thesis proposes using the variance in the *charge* that flows through the synapse, rather than the current. The charge will be less influenced by cable filtering, but its inter-trial variance will still encode in some way the size and number of ion channels.

1.3 Summary

Features of the synapse, such as the single channel conductance, can be estimated by analysing the mean and variance of the current through the synapse. The current, however, becomes distorted as it travels through the dendrite to the recording electrode. This affects the results of the standard current-based noise analysis. The charge that flows through the synapse is

less affected by the cable filtering, and so may provide a more robust way of analysing distal synapses.

Chapter 2

Simulating a simple O $\longrightarrow$ C synapse

2.1 Introduction

To produce a charge-based analysis of a synapse, the effect of different channel features on the charge variance and mean must be understood. The behaviour of a channel depends, at the most basic level, on the structure of the proteins it is built from. It is these structures that define how the channel opens and closes. Channels can be gated in different ways, for instance, some are opened when bound to a neurotransmitter, while others are opened (or closed) by changes in membrane voltage. Often channels can enter a 'desensitised' state, from which they need to be 'reset' before opening again.

A useful way to model a channel is to consider it to have several states, such as the desensitised state mentioned above. The transition between states can be described by the rate at which transitions occur. These rates can be dependent on the concentration of neurotransmitter or the membrane voltage.

The transition *rates* are often described using a matrix, W. If the matrix describes the *probability* of a transition, the letter M is used instead.

Later, in section 2.4.2, we consider a channel with the most simple state diagram possible. One with just an open state and a closed state. However, we start, in section 2.2 by using a 3x3 transition matrix to illustrate how to use, manipulate and model the state kinetics.

2.2 The Markov Model

2.2.1 The Markov Matrix

A channel's state is described by the vector **s**. For instance, if there were three states, and the channel was in the first one:

$$\mathbf{s} = \begin{bmatrix} 1 \\ 0 \\ 0 \end{bmatrix} \tag{2.1}$$

A markov matrix M describes the probability of the channel moving from one state to another during a certain time interval. For example, if

$$M = \begin{bmatrix} 0.3 & 0.2 & 0.4 \\ 0.1 & 0.4 & 0.1 \\ 0.6 & 0.4 & 0.5 \end{bmatrix} \tag{2.2}$$

then the probability of the channel being in each state after a time step is equal to:

$$M\mathbf{s} = \mathbf{p} \tag{2.3}$$

Which means, in our example, **p** equals:

$$\begin{bmatrix} 0.3 & 0.2 & 0.4 \\ 0.1 & 0.4 & 0.1 \\ 0.6 & 0.4 & 0.5 \end{bmatrix} \begin{bmatrix} 1 \\ 0 \\ 0 \end{bmatrix} = \begin{bmatrix} 0.3 \\ 0.1 \\ 0.6 \end{bmatrix} \tag{2.4}$$

So the channel has a 30% chance of being in the first state, 10% chance of being in the second state, and a 60% of being in the third state. Notice that M's columns must each add up to one, to ensure that the probability vector adds up to one.

2.2.2 Open to Closed Kinetics

To model a real ion channel the Markov Matrix M would have to change, depending on the amount of neurotransmitter or membrane voltage. In order to simplify the analysis, the matrix has been made constant. This simplification may be acceptable, as the neurotransmitter is only briefly present in the synaptic cleft, so for the majority of the time, the matrix will be constant. To calculate the charge in the charge-based analysis later, the current is integrated over an infinite period. For this to be possible, the current flow must approach zero over time. This means the channel must close, and remain closed. Because M is fixed, the only behaviour that can be modelled is for the channel to move from open states to closed states, so in this chapter and the next the analysis will be restricted to Open to Closed kinetics.

2.2.3 Time Steps

The markov matrix, M, describes the probability of a transition in a unit of time. To calculate the probability, over a different period, we can raise the markov matrix to the power of the length of this time interval. For instance if our time step is 2 seconds, then M would need to be squared,

$$M^2 = \begin{bmatrix} 0.35 & 0.3 & 0.34 \\ 0.13 & 0.22 & 0.13 \\ 0.52 & 0.48 & 0.53 \end{bmatrix} \tag{2.5}$$

2.2.4 Current

Each state has a certain current associated with it, for instance the first two states might be closed and allow 0 Amps to flow, while the third state might be open and allow 1pA through. The current that can flow in each state is defined by the vector **m**, which in this example would equal:

$$\mathbf{m} = \begin{bmatrix} 0 \\ 0 \\ 10^{-12} \end{bmatrix} \tag{2.6}$$

The current flow through a channel is given by the dot product of the state vector, **s** and the current vector, **m**. For our example the current flow would be:

$$\mathbf{s}.\mathbf{m} = \begin{bmatrix} 1 \\ 0 \\ 0 \end{bmatrix} . \begin{bmatrix} 0 \\ 0 \\ 10^{-12} \end{bmatrix} = 0 \text{ Amps} \tag{2.7}$$

2.2.5 Creating the next State

Equation 2.3 gives the probabilities **p** of entering different states in the next time step. However, to model the channel, this probability distribution needs to be sampled, and a definite state must be selected. This new state is used to create the new state vector **s**.

From the example above,

$$\mathbf{p} = \begin{bmatrix} 0.3 \\ 0.1 \\ 0.6 \end{bmatrix} \tag{2.8}$$

A state must be randomly selected with these probabilities. I.e. with 30% chance of picking the first state, etc. Below, an outline of the implementation is described. This was used in the matlab model to generate a simulated signal of the synaptic noise.

The implementation starts by picking a random number r, from zero to one. This is compared with the first probability in the vector, p_1 (0.3 in the example above). If r is greater than

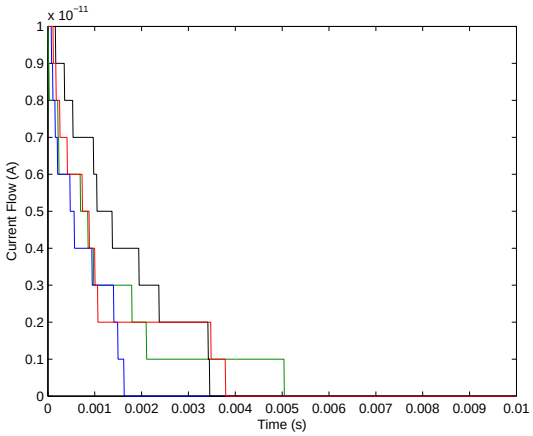

Figure 2.1: *Four examples of cable current using the O → C kinetics.*

p_1, then it is subtracted from r, i.e.: $r \rightarrow r - p_1$. It is then compared to the next probability p_2. This is repeated for each probability. If, for any state, i, $r < p_i$, state i is chosen as the next state the channel will enter.

From our earlier example:

$$\mathbf{p} = M\mathbf{s} = \begin{bmatrix} 0.3 \\ 0.1 \\ 0.6 \end{bmatrix} \tag{2.9}$$

Selecting a random number, let $r = 0.35$. First compare it with $p_1 = 0.3$. r is greater so let $r \rightarrow r - 0.3 = 0.05$. Next it is compared with $p_2 = 0.1$. r is now smaller than p_2, so we make 2 the new state.

This calculation was repeated for each channel at each time step. By applying this to the simple open → closed model, the expected decay in the number of open channels was produced (figure 2.1). The source code for this algorithm can be seen in appendix C, in listing 3.

2.3 Alternative Calculation

2.3.1 Sample Rate vs Runtime

The simulation models up to 1,000 channels over 10,000 iterations. At each time step, the calculation of the new states must be repeated for all channels. This can be quite slow with many channels. To reduce the runtime, the time steps were made larger, but this was found to cause more than one channel to transition at any time, which risked altering the noise statistics.

2.3.2 Modelling channels simultaneously

Another option was to model all the channels simultaneously. By combining all the different channel transitions into a single time step, the run time could be improved. To do this, the state

vector **s** was used to describe the *number of channels* in each state, rather than the state of just one channel. With $\mathbf{s}_i$ channels in state *i*, and with a probability M_{ji} of each of these channels entering state j, the number that do enter state j from state i can be modelled using the *binomial distribution*.

2.3.3 Implementation

To improve the runtime of the algorithm, the following algorithm was implemented.

1. Let N equal M, but with its diagonal set to zero.
2. Adjust for the step size (by raising to the necessary power).
3. Sample from the binomial distribution to find the number of transitions to each state. This describes the transitions that will occur in the next time step and is recorded in the transition matrix, T:
$$T_{ji} = B(\mathbf{s}_i, N_{ji}) \tag{2.10}$$
4. Sum the columns of T, and subtract these from the diagonal of T.
5. Sum the rows of T, and add to **s**.

2.3.4 Example

Below is an example of the implementation. First, let:

$$\mathbf{s} = \begin{bmatrix} 5 \\ 4 \\ 1 \end{bmatrix} \tag{2.11}$$

1. Using for N, the matrix M as defined in equation 2.2, with its diagonal equal to zero:
$$N = \begin{bmatrix} 0 & 0.2 & 0.4 \\ 0.1 & 0 & 0.1 \\ 0.6 & 0.4 & 0 \end{bmatrix} \tag{2.12}$$
2. Adjust for the step size: We assume for this example that the step size is one second, so N remains unchanged.
3. We can now find T by sampling from the binomial distribution:
$$T = \begin{bmatrix} 0 & B(4,0.2) & B(1,0.4) \\ B(5,0.1) & 0 & B(1,0.1) \\ B(5,0.6) & B(4,0.4) & 0 \end{bmatrix} \tag{2.13}$$

The distributions are sampled, producing (for example):

$$T = \begin{bmatrix} 0 & 0 & 1 \\ 1 & 0 & 0 \\ 4 & 2 & 0 \end{bmatrix} \tag{2.14}$$

4. Subtracting the columns from the diagonals to take into account the removal of channels from their original states:

$$\begin{bmatrix} -5 & 0 & 1 \\ 1 & -2 & 0 \\ 4 & 2 & -1 \end{bmatrix} \tag{2.15}$$

5. Finally sum the rows to find the change in the number of channels in each state:

$$\begin{bmatrix} -4 \\ -1 \\ 5 \end{bmatrix} \tag{2.16}$$

This can be added to the original state vector, to find the new number of channels in each state:

$$\mathbf{s}' = \begin{bmatrix} 5 \\ 4 \\ 1 \end{bmatrix} + \begin{bmatrix} -4 \\ -1 \\ 5 \end{bmatrix} = \begin{bmatrix} 1 \\ 3 \\ 6 \end{bmatrix} \tag{2.17}$$

2.3.5 Adjustments

The method described above, using the binomial distribution to estimate the number of transitions, may not always be successful. Critically, the number transferred from one state could be more than the number in that state. This can happen, for example, when two transitions from a state, s_i, each take more than half the channels in that state. If this happens the state will have a negative occupancy. I.e. a negative number of channels will be in that state. This is obviously impossible. With small time steps this error is rare, as the probability of more than one transition each time step is already kept low to avoid altering the noise. If the error does happen the result from the calculation is ignored and the binomial samples are taken again.

2.3.6 Speedup

Although it appears this should provide a reasonable speedup over modelling the channels separately, the matlab binomial sampling function `binornd` doesn't take a fixed length of time to run. Instead it takes $\Theta(n)$ time, due to a loop that iterates n times, exactly the same asymptotic time the separate channel model would take. As a result, this implementation did not provide a substantial speedup.

1. Sample many trials of the same impulse being applied.
2. Calculate the mean current, $\langle I(t) \rangle$, and its variance, $\sigma_I^2(t)$, for each sample time t.
3. Plot the variance, $\sigma_I^2(t)$, against the mean, $\langle I(t) \rangle$.
4. Fit a parabola to the curve.
5. Use the curve parameters to calculate features of the synapse.

Figure 2.2: *How to apply the Current Based Noise Analysis*

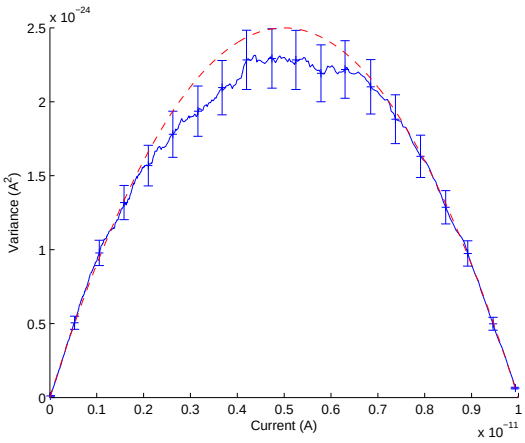

Figure 2.3: *Current-based noise analysis, The initial gradient is equal to 1pA, the single channel current, as expected. The second intersection is at 10 times this, also as expected, as 10 is the number of channels used. (1000 iterations were taken. Error bars are 95% confidence intervals). Dashed line indicates expected result.*

2.4 Noise Analysis

2.4.1 *Current Based* Noise Analysis

Regardless of the implementation, using the Open to Closed kinetics will produce outputs such as those in figure 2.1. By repeating the experiment many times the mean and variance in the current can be found for each time step. A graph such as that in figure 2.3 can then be plotted. The initial gradient of the mean-variance graph gives the single-channel current of 1pA. The stages used in current-based noise analysis are listed in figure 2.2.

2.4.2 *Charge Based* Noise Analysis

The channels are assumed to have the same single-channel conductance. This means they each allow the same current to flow when open. The total charge that flows from a time t to ∞ is equal to the integral of the current from t onwards.

The charge for any time t for a particular trial can be compared to the charge at time t in

1. Sample many trials of the same impulse being applied.
2. Find the charge for a time t by integrating the current from the time t to the end of the trial.
3. Calculate this integral for all times t from the start to the end of the trial.
4. Compare these integrals between trials, and calculate the mean charge, $\langle Q(t) \rangle$, and its variance, $\sigma^2_Q(t)$, for each sample time t.
5. Plot the variance, $\sigma^2_Q(t)$, against the mean, $\langle Q(t) \rangle$.
6. Fit a parabola to the curve.
7. Use the curve parameters to calculate features of the synapse.

Figure 2.4: *How to apply the Charge Based Noise Analysis*

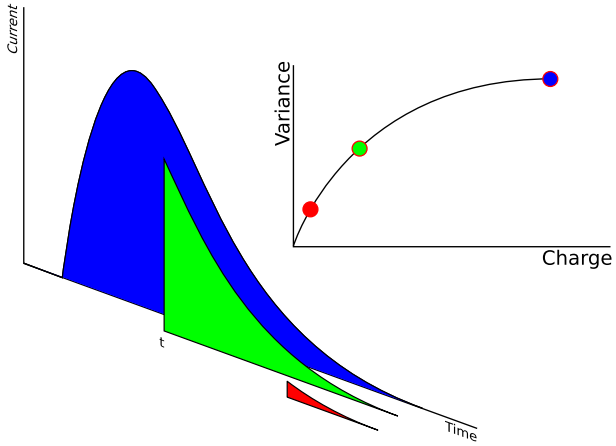

Figure 2.5: *The charge is calculated by integrating the current over time, from a time t to infinity.*

the other trials, and the mean and variance at t can be calculated. The mean and variance for values of t from 0 to the end of the trial are found and the two can be plotted against each other (figure 2.5), in a similar way to how the mean and variance of the current were plotted.

The shape of this curve can be considerably more complex than the current-variance curve. However, for the simple open to closed kinetics, the curve remains a parabola. Figure 2.4 summarises the stages in the charge based analysis.

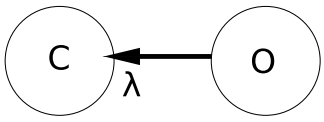

Figure 2.6: *Simple Open to Closed kinetics. λ is the rate at which the channel closes.*

2.4.3 Deriving the Variance of the Charge

Consider one channel for the moment. The mean and variance of the charge that flows through this channel are proportional to the mean and variance of the period of time it's open for.

Initially assume the channel is open to start with, and it will close at some time in the future, with a rate constant λ. I.e. this is a simple open to close channel, which is initial open and will close at some point (figure 2.6).

The time the channel remains open can be modelled as a Poisson Distribution. The probability of being open after t seconds is equivalent to the probability that no occurrences of the event occur from time zero to time t. So, using the Poisson Distribution, the probability of it being open is:

$$P_{open} = \frac{(\lambda t)^k e^{-\lambda t}}{k!} = e^{-\lambda t} \tag{2.18}$$

Where k is the number of occurrences of the event (in this case 0), λ is the rate (s^{-1}) and t is the time interval.

Closing at time t, leaves a probability *density* of:

$$p_{open\ until\ t} = \lambda e^{-\lambda t} \tag{2.19}$$

From this definition, the first and second moments of expected closing times can be found:

$$\langle t \rangle = \int_0^\infty t\lambda e^{-\lambda t}\, dt = \left[-e^{-\lambda t}\left(t + \frac{1}{\lambda}\right)\right]_0^\infty = \frac{1}{\lambda} \tag{2.20}$$

$$\begin{aligned} \langle t^2 \rangle &= \int_0^\infty t^2 \lambda e^{-\lambda t}\, dt \\ &= \left[-e^{-\lambda t}\left(t^2 + \frac{2}{\lambda}t + \frac{2}{\lambda^2}\right)\right]_0^\infty \\ &= \frac{2}{\lambda^2} \end{aligned} \tag{2.21}$$

If a time t_0 has elapsed, then some of the channels will already have closed. We assume a channel has a probability p of still being open after t_0 seconds. Note, the initial time is still taken to be zero in the following integrals, to ease the integration. This does not affect the result, because the stochastic closing behaviour is dependent purely on the closing rate. The mean and variance of the channel's charge from any time to infinity can now be found. Note that, in the literature, a 'survival rate' τ is often used, instead of $\frac{1}{\lambda}$. This has been substituted in.

The first and second moments of charge, q, for a single channel are dependent on the single channel current, i_0, and the time the channel is open, t. The mean length of time the channel is open for, multiplied by the current that flows through it while open, gives the mean charge, if

it is open to start with. This has to be multiplied by the probability, p, of it being open at the start:

$$\langle q \rangle = \langle t i_0 \rangle p = p\tau i_0 \tag{2.22}$$

The second moment of charge $\langle q^2 \rangle$ can be found in a similar way. Using equation 2.21, but applying it to the current τi_0 rather than time t, gives:

$$\langle q^2 \rangle = \langle (t i_0)^2 \rangle p = 2p(\tau i_0)^2 \tag{2.23}$$

So the variance in the amount of charge that flows through a channel, from any time, with a probability p of the channel being open is:

$$\begin{aligned} s_q^2 &= \langle q^2 \rangle - \langle q \rangle^2 \\ &= 2p(\tau i_0)^2 - (p\tau i_0)^2 \\ &= (\tau i_0)^2 (2p - p^2) \end{aligned} \tag{2.24}$$

The mean and variance of the charge through all N channels, Q, is the sum of the individual means and variances respectively. This assumes that the behaviour of individual channels is mutually uncorrelated.

$$\bar{Q} = \langle Q \rangle = \langle q \rangle N = pN\tau i_0 \tag{2.25}$$

$$s_Q^2 = s_q^2 N = (\tau i_0)^2 N (2p - p^2) \tag{2.26}$$

2.4.4 Finding the shape of the Charge-Variance curve

Plotting the variance of the charge against its mean produces a parabola, with a peak where $p = 1$. I.e. where:

$$\bar{Q} = N\tau i_0 \tag{2.27}$$

and

$$s_Q^2 = (\tau i_0)^2 N \tag{2.28}$$

To find the initial gradient, differentiate both mean and variance w.r.t. p:

$$\frac{d\bar{Q}}{dp} = \frac{d}{dp} i_0 \tau N p = i_0 \tau N \tag{2.29}$$

$$\frac{d\bar{s_Q^2}}{dp} = \frac{d}{dp}(i_0\tau)^2 N(2p-p^2) = (i_0\tau)^2 N(2-2p) \tag{2.30}$$

So the gradient is:

$$\frac{(i_0\tau)^2 N(2-2p)}{N i_0 \tau} = i_0\tau(2-2p) \tag{2.31}$$

The gradient at $p = 0$ is therefore:

$$2i_0\tau \tag{2.32}$$

This was tested using the unfiltered noise analysis matlab code, developed in the first part of this chapter. The single channel conductance was set to 1 pA and the closing rate (λ) set to 0.25 per millisecond. This means $\tau = \frac{1}{0.25\times10^3} = 4\times10^{-3}$s. It was also defined that 100 channels are initially open. From these values some expected values can be calculated for the graph.

Using equation 2.27, The peak of the graph may be expected where $\bar{Q}$ is:

$$\begin{aligned} \bar{Q} &= N\tau i_0 \\ &= 100\times4\times10^{-3}\times10^{-12} \\ &= 4\times10^{-13}C. \end{aligned} \tag{2.33}$$

from equation 2.28, the peak variance should be where:

$$\begin{aligned} s_Q^2 &= (\tau i_0)^2 N \\ &= (4\times10^{-3}\times10^{-12})^2\times100 \\ &= 1.6\times10^{-27}C^2. \end{aligned} \tag{2.34}$$

Fitting the quadratic $y = ax^2 + bx + c$ to the data (as in figure 2.7), suggests the peak is at mean charge:

$$-b/2a = -8.01\times10^{-15}/(2\times-0.0104) = 3.85\times10^{-13}C \tag{2.35}$$

and variance: $1.54\times10^{-27}C^2$.

which closely match the expected values calculated above.

The gradient at $p = 0$ is 8.01×10^{-15}C, which is very close to our expected value: $2\tau i_0 = 8\times10^{-15}$C.

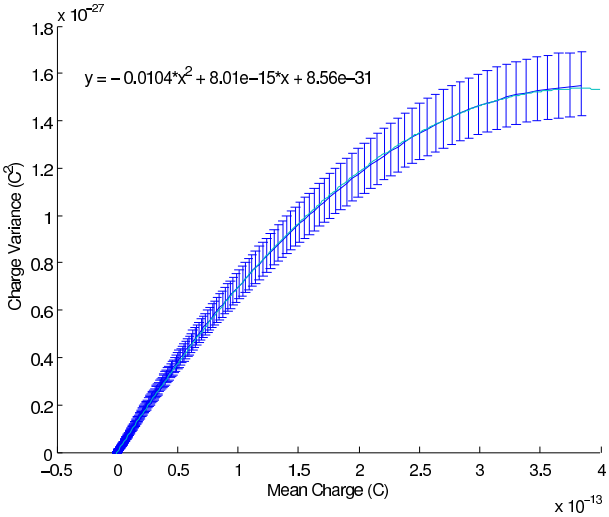

Figure 2.7: *Charge-based analysis showing a typical plot of mean vs variance. 1000 samples have been taken and the error bars indicate 95% confidence intervals.*

2.5 Summary

The charge-based analysis has been shown to work for simple Open → Closed kinetics. It successfully predicted the channel size and number using the initial gradient and axis-intersect. Solving for more complex kinetics is more complicated, and the analysis still must be proved to deal with cable filtering.

2.6 Note about Confidence Intervals

The confidence intervals drawn in these plots are a measure of the standard error of the estimate of the population variance. Originally the expression for these confidence intervals was taken from P. Wildman's derivation[24]. This suggested that the confidence intervals for the population variance were:

$$\frac{(n-1)s^2}{\chi_R^2} < \sigma^2 < \frac{(n-1)s^2}{\chi_L^2} \tag{2.36}$$

Where χ^2 is the chi-squared distribution, n is the number of samples, s^2 is the sample variance and σ^2 is the population variance.

This can be calculated using another expression found in Practical Physics[20]. This expression gives the variance, ς^2, of the estimated population variance (σ^2):

$$\langle \varsigma^2 \rangle = \frac{2}{n-1}(s^2)^2 \tag{2.37}$$

Both these techniques result in similar errorbars, although the former will be slightly more accurate as it takes into account their slight non-symmetry. However, the latter expression is

used as it doesn't require calculating χ^2 and so is considerably quicker.

Chapter 3

Charge and Variance for more Complex Channels

3.1 Deriving Variance and Charge for different channel kinetics

3.1.1 The model

The following derivation is largely the work of Adam Barrett and Mark van Rossum.

The channel dynamics are still described using a Markov process, but the matrix is now a description of the rate of change between states, W. It is similar to using T to calculate the number of transitions. The rate of change can now be written as:

$$\frac{d\mathbf{s}(t)}{dt} = W\mathbf{s}(t) \tag{3.1}$$

From linear algebra, the solution to this differential equation is:

$$\mathbf{s}(t) = VD(e^{\lambda t})V^{-1}\mathbf{s}(0) \tag{3.2}$$

where V is a matrix formed from the column eigenvectors of W and $D(e^{\lambda t})$ is a diagonal matrix with $e^{\lambda_i t}$ along the diagonal, where λ_i is the ith eigenvalue of W.

Each state has a particular current associated with it, which is represented by the vector $\mathbf{m}$. For example if the first state is the open state, and allows 20pA to flow, and the second state is closed, $\mathbf{m}$ would be:

$$\mathbf{m} = \begin{bmatrix} 20 \times 10^{-12} \\ 0 \end{bmatrix} \tag{3.3}$$

The mean current at any time, t, is equal to the current flow for the channel's state. So if the channel is in the second state in the example above, then the channel will have no current flow. This can be expressed mathematically as the dot product between the current vector and the state vector:

$$\langle I(t) \rangle = \mathbf{m}^\top \mathbf{s}(t) \tag{3.4}$$

Substituting equation 3.2 into 3.4, we find that the total mean current, $\langle I(t)\rangle$ at time t:

$$\langle I(t)\rangle = \mathbf{m}^\top V D(e^{\lambda t}) V^{-1}\mathbf{s}(0) \tag{3.5}$$

3.1.2 Charge

The expression for the charge that accumulates from a time t_0 to ∞, is the integral of $I(t)$ from t_0 to ∞:

$$\begin{aligned}\langle Q\rangle(t_0) &= \int_{t_0}^{\infty}\langle I(t)\rangle dt = \int_{t_0}^{\infty}\mathbf{m}^\top V D(e^{\lambda t})V^{-1}\mathbf{s}(0)\\ &= \left[\mathbf{m}^\top V D(\frac{e^{\lambda t}}{\lambda})V^{-1}\mathbf{s}(0)\right]_{t_0}^{\infty}\end{aligned} \tag{3.6}$$

Note that as $t\to\infty$, $e^{\lambda t}\to 0$, if $\forall\, i,\ |\lambda_i|<0$. Therefore:

$$\langle Q\rangle(t_0) = -\mathbf{m}^\top V D(\frac{e^{\lambda t_0}}{\lambda})V^{-1}\mathbf{s}(0) \tag{3.7}$$

3.1.3 Current Autocorrelation

Remembering that $\mathbf{s}_i(t)$ describes the number of channels in state i at time t, the probability of entering state j from state i in time $(t'-t)$ is expressed as $P(j,t'|i,t)$, and so the number of expected transitions from state i to state j is: $P(j,t'|i,t)\mathbf{s}_i(t)$. The product of the current before and after the transition is then: $\left(\mathbf{m}_j^\top P(j,t'|i,t)\mathbf{m}_i^\top\right)\mathbf{s}_i(t)$. This can be summed over all the possible pairs of states, giving the total mean change in current from time t to time t', this is the autocorrelation.

$$\langle I(t)I(t')\rangle = \sum_{ij}\mathbf{m}_j^\top P(j,t'|i,t)\mathbf{m}_i^\top\mathbf{s}_i(t) \tag{3.8}$$

The probability of the transition from i to j is expressed in the transition matrix: W_{ji}. So the probability of such a transition in time $t'-t$, can be found using part of equation 3.2: $\left[VD(e^{\lambda(t'-t)})V^{-1}\right]_{ji}$.

Substituting this into equation 3.8, and substituting in 3.2,

$$\langle I(t)I(t')\rangle = \sum_{ij}\mathbf{m}_j^\top\left[VD(e^{\lambda(t'-t)})V^{-1}\right]_{ji}\mathbf{m}_i^\top\left[VD(e^{\lambda t})V^{-1}\mathbf{s}(0)\right]_i \tag{3.9}$$

The summation can be written as matrix operations:

$$\langle I(t)I(t')\rangle = \mathbf{m}^\top V D(e^{\lambda(t'-t)})V^{-1}D(\mathbf{m})VD(e^{\lambda t})V^{-1}\mathbf{s}(0) \tag{3.10}$$

3.1.4 Example: The Current Variance

The variance in the current can be derived from equation 3.10:

$$\langle I(t)^2\rangle = \langle I(t)I(t)\rangle$$

$$
\begin{aligned}
&= \mathbf{m}^\top VD(e^{\lambda \times 0})V^{-1}D(\mathbf{m})VD(e^{\lambda t})V^{-1}\mathbf{s}(0) \\
&= \mathbf{m}^\top VD(1)V^{-1}D(\mathbf{m})VD(e^{\lambda t})V^{-1}\mathbf{s}(0) \\
&= \mathbf{m}^\top D(\mathbf{m})\mathbf{s}(t) \\
&= \mathbf{m}_2^\top \mathbf{s}(t)
\end{aligned}
\tag{3.11}
$$

Where $(\mathbf{m}_2)_i$ is defined to be $\mathbf{m}_i^2$.

The variance in the current is therefore:

$$\sigma_I^2 = \langle I^2 \rangle - \langle I \rangle^2 = \mathbf{m}_2^\top \mathbf{s}(t) - \left[\mathbf{m}^\top \mathbf{s}(t)\right]^2$$

as expected.

3.1.5 Charge Variance

The second moment of Q is:

$$\langle Q^2 \rangle (t_0) = 2 \int_{t_0}^{\infty} \int_{t}^{\infty} \langle I(t) I(t') \rangle \; dt' \; dt \tag{3.12}$$

The factor of 2 is needed because the double integral only covers t, t' pairs where $t \geq t'$.

Substituting equation 3.10 and integrating

$$
\begin{aligned}
\langle Q^2 \rangle (t_0) \qquad &= 2 \int_{t_0}^{\infty} \int_{t}^{\infty} \mathbf{m}^\top VD(e^{\lambda(t'-t)})V^{-1}D(\mathbf{m})VD(e^{\lambda t})V^{-1}\mathbf{s}(0) \; dt' \; dt \\
&= 2 \int_{t_0}^{\infty} \left[\mathbf{m}^\top VD(\frac{e^{\lambda(t'-t)}}{\lambda})V^{-1}D(\mathbf{m})VD(e^{\lambda t})V^{-1}\mathbf{s}(0) \right]_t^{\infty} \; dt \\
&= -2 \left[\mathbf{m}^\top VD(\frac{1}{\lambda})V^{-1}D(\mathbf{m})VD(\frac{e^{\lambda t}}{\lambda})V^{-1}\mathbf{s}(0) \right]_{t_0}^{\infty} \\
&= 2\mathbf{m}^\top VD(\frac{1}{\lambda})V^{-1}D(\mathbf{m})VD(\frac{e^{\lambda t_0}}{\lambda})V^{-1}\mathbf{s}(0)
\end{aligned}
\tag{3.13}
$$

This expression and equation 3.6 can be used to find the variance of the charge, which can be calculated with the usual definition, by substituting the above expressions:

$$\sigma_Q^2(t_0) = \langle Q^2 \rangle (t_0) - [\langle Q \rangle (t_0)]^2 \tag{3.14}$$

3.2 Charge-Variance Curves

3.2.1 Channel Dynamics

Using equation 3.14 and 3.7 the charge-variance curves can be plotted using different channel dynamics. An unlimited number of possible state diagrams could be considered, but in the following section only four simple models have been calculated. If there is only one open state the resulting curve will be a parabola. This is proved below.

3.2.2 Single Open State

If there is just one open state, then $\mathbf{m}$ will be a column vector of zeros, with one i_0 at $\mathbf{m}_j$:

$$\mathbf{m} = \begin{bmatrix} 0 \\ \vdots \\ i_0 \\ \vdots \\ 0 \end{bmatrix} \tag{3.15}$$

And so $D(\mathbf{m})$ will be a matrix of zeros, with one i_0 at position $D(\mathbf{m})_{jj}$.

The mean charge, as given by equation 3.7 is:

$$\langle Q \rangle(t_0) = -\mathbf{m}^\top V D(\frac{e^{\lambda t_0}}{\lambda}) V^{-1} \mathbf{s}(0) \tag{3.16}$$

The equation for the second moment of charge (equation 3.13) can be considered in two parts:

$$\langle Q^2 \rangle(t_0) = \left[2\mathbf{m}^\top V D(\frac{1}{\lambda}) V^{-1} \right] \left[D(\mathbf{m}) V D(\frac{e^{\lambda t_0}}{\lambda}) V^{-1} \mathbf{s}(0) \right] \tag{3.17}$$

By comparing this equation with that for mean charge, it can be observed that the second part of the equation will equal a column vector of zeros, with the mean charge at position j:

$$D(\mathbf{m}) V D(\frac{e^{\lambda t_0}}{\lambda}) V^{-1} \mathbf{s}(0) = \begin{bmatrix} 0 \\ \vdots \\ \langle Q(t_0) \rangle \\ \vdots \\ 0 \end{bmatrix} \tag{3.18}$$

The first part of 3.17 will be a row-vector that is independent of t. I.e. of the form:

$$\mathbf{m}^\top A = \mathbf{m}^\top 2 V D(\frac{1}{\lambda}) V^{-1} \tag{3.19}$$

Where $A = 2VD(\frac{1}{\lambda})V^{-1}$. Combining these two expressions, the second moment can be expressed as:

$$\langle Q^2(t_0) \rangle = \mathbf{m}^\top A \begin{bmatrix} 0 \\ \vdots \\ \langle Q(t_0) \rangle \\ \vdots \\ 0 \end{bmatrix} = \begin{bmatrix} 0 & \dots & i_0 & \dots & 0 \end{bmatrix} A \begin{bmatrix} 0 \\ \vdots \\ \langle Q(t_0) \rangle \\ \vdots \\ 0 \end{bmatrix} = i_0 A_{jj} \langle Q(t_0) \rangle \tag{3.20}$$

The charge variance is defined in equation 3.14 as:

$$\sigma_Q^2(t_0) = \langle Q^2 \rangle(t_0) - [\langle Q \rangle(t_0)]^2 \tag{3.21}$$

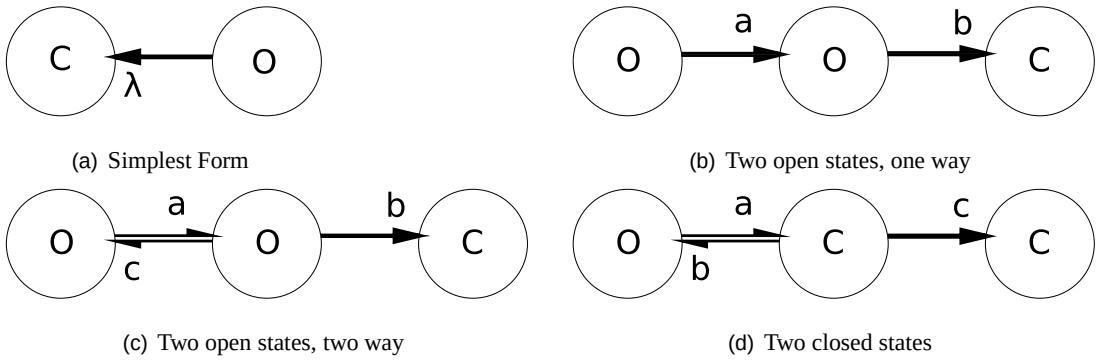

(a) Simplest Form (b) Two open states, one way

(c) Two open states, two way (d) Two closed states

Figure 3.1: *Possible simple examples of channel markov kinetics. The letters describe various transition rates between states.*

Substituting the new definition for $\langle Q^2 \rangle$ from equation 3.20 into equation 3.21, gives:

$$\sigma_Q^2(t_0) = [i_0 A_{jj} \langle Q(t_0) \rangle] - [\langle Q \rangle (t_0)]^2 \tag{3.22}$$

Because $i_0 A_{jj}$ is a constant this is a quadratic equation; so the variance, plotted against the charge will form a parabola.

Thus markov models with a single open state will always have a parabolic charge-variance curve.

3.2.3 Models Calculated

Four models of channel kinetics were examined and are illustrated in figure 3.1.

3.2.4 O $\rightarrow$ C

The transition matrix W for the simplest dynamics, figure 3.1(a), is:

$$\begin{bmatrix} -a & 0 \\ a & 0 \end{bmatrix} \tag{3.23}$$

The curve is a parabola, with a peak at: $\left(\frac{1}{a}, \frac{1}{a^2}\right)$ and an initial gradient of $\frac{2}{a}$.

3.2.5 O $\rightarrow$ O $\rightarrow$ C

Next, a second open state was added (figure 3.1(b)). This no longer forms a parabola (figure 3.2). However, as expected, when $a >> b$ or $b >> a$ the curve approximates a parabola (black line, figure 3.2), with the same features as the simple $O \rightarrow^{\alpha} C$ graph, in which $\alpha = min(a,b)$. The time spent in one state is much less than the time spent in the other, making the kinetics approach $O \rightarrow C$.

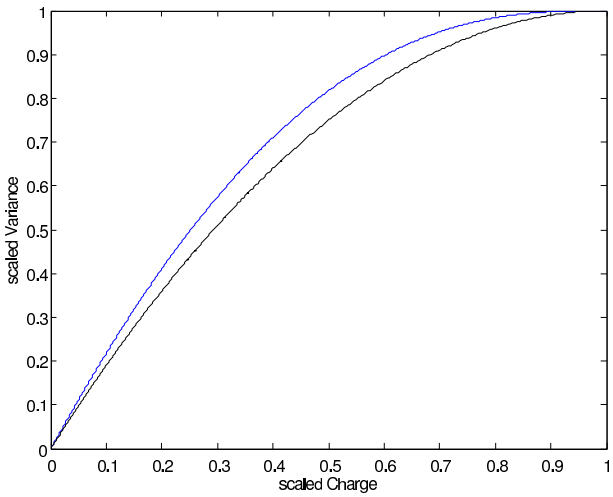

Figure 3.2: *Scaled Charge/Variance graph showing how the shape changes with a and b. The black line is the parabola, the blue line is the charge-variance graph when $a \approx b$.*

The transition matrix is:

$$W = \begin{bmatrix} -a & 0 & 0 \\ a & -b & 0 \\ 0 & b & 0 \end{bmatrix} \tag{3.24}$$

The peak of the curve is at: $\left(\frac{1}{a}+\frac{1}{b}, \frac{a^3-a^2b+ab^2-b^3}{a^3b^2-a^2b^3}\right)$. And the curve has an initial gradient: $\frac{2}{min(a,b)}$. This rather unexpected result is proved in appendix D.

3.2.6 O ↔ O → C

Another transition was added (figure 3.1(c)), allowing the channel to re-enter the first state, changing the transition matrix to:

$$W = \begin{bmatrix} c-a & a-c & 0 \\ a-c & c-a-b & 0 \\ 0 & b & 0 \end{bmatrix} \tag{3.25}$$

This has a peak where the charge, $Q = \frac{2a+b-2c}{ab-bc}$, the expression for the variance at this point is too large to usefully express.

The initial gradient is still $\frac{2}{min(a,b)}$, and it again does not form a parabola.

3.2.7 O ↔ C → C

More than one open state appears to cause the curve to become non-parabolic. The above example was modified to just have one open state (figure 3.1(d)). This formed a parabola, as proved in section 3.2.2, with a peak at $\left(\frac{a+c}{bc}, \frac{(a+c)^2}{(bc)^2}\right)$, and an initial gradient of $2\frac{a+c}{bc}$. This model will be useful later, when simplifying the AMPA receptor kinetic model.

3.3 Limitations

3.3.1 Steady State

The technique described in this chapter is an analytical solution for finding the charge's mean and variance. The technique does have limitations. The most important is that it needs the channel's steady state solution to be closed. A real channel, however, will go from closed to open, then close again as the transition matrix changes. This is possibly a problem with the charge-based concept in general, which may rely on the transition rates being constant.

3.3.2 Transition Rates

Without constant transition rates, the theoretical values for charge and variance will be difficult to find. It may be that the critical transitions that need to be modelled are constant (rather than dependent on ligand-binding or voltage) in which case this technique may work.

3.3.3 Complexity

The state-diagrams examined only have a maximum of three states, while real channels may have dozens. Modelling them in the same way will cause the expressions for the curve peak, and initial gradient to become unusable. For instance a simple AMPA receptor model was tested in mathematica, and the expression for the variance peak had over 100 terms.

3.4 Fitting Parabolas

3.4.1 Necessity

In the following chapters, many charge-variance and current-variance plots will be generated. Fitting each of these with a parabola will be necessary to find the initial gradient and possible peak. *Matlab* has the `polyfit` function, which can be used, however this has two drawbacks:

- It does not take into account the confidence intervals of each sample.
- It does not provide confidence intervals for the parameters it calculates.

Below is a derivation of the method for finding the three parameters that define a parabola, using standard linear regression.

3.4.2 Finding the parameters

A plot has a set of points (x_i, y_i) which a parabola may be fitted to. The parabola is defined by three parameters, so the expected y value for any x_i is:

$$e_i = a + bx_i + cx_i^2 \tag{3.26}$$

We can write this as:

$$e_i = \mathbf{w}^\top \phi \tag{3.27}$$

where:

$$\mathbf{w} = \begin{bmatrix} a \\ b \\ c \end{bmatrix}$$

and

$$\phi = \begin{bmatrix} 1 \\ x_i \\ x_i^2 \end{bmatrix}$$

The sum squared error between the estimate **e** and the data **y** can be calculated. The probability that this error is due to random variance is calculated using the χ^2 distribution, for a particular set of parameters, **w**:

$$\chi^2(\mathbf{w}) = \sum_{i=1}^{N} \left(\frac{y_i - \mathbf{w}^\top \phi_i}{\sigma_i} \right)^2 \tag{3.28}$$

Where σ_i is the standard error of sample i. χ^2 is differentiated with respect to $\mathbf{w_k}$, and this derivative is set equal to zero:

$$0 = \frac{\partial \chi^2(\mathbf{w})}{\partial \mathbf{w}} = -2 \sum_{i=1}^{N} \frac{y_i \phi_i}{\sigma_i^2} + 2 \sum_{i=1}^{N} \frac{2\phi_i (\phi_i)^\top \mathbf{w}}{\sigma_i^2} \tag{3.29}$$

By solving for **w** the parameters than minimise the sum square error can be found:

$$\mathbf{w} = \left(\sum_{i=1}^{N} \frac{\phi_i (\phi_i)^\top}{\sigma_i^2} \right)^{-1} \sum_{i=1}^{N} y_i \phi_i \tag{3.30}$$

Note that this fit takes into account the variance of the samples. Figure 3.3 illustrates how this can be important.

3.4.3 Finding the parameters' confidence intervals

The variance (σ_f^2) in the value of any function f is:

$$\sigma_f^2 = \sum_{k=1}^{N} \sigma_k^2 \left(\frac{\partial f}{\partial y_k} \right)^2 \tag{3.31}$$

This rule can be applied to the equation for **w** (3.30). First differentiate with respect to y_k:

$$\frac{\partial \mathbf{w}}{\partial y_k} = \left(\sum_{i=1}^{N} \frac{\phi_i (\phi_i)^\top}{\sigma_i^2} \right)^{-1} \frac{\phi_k}{\sigma_k^2} \tag{3.32}$$

Then substitute in (3.32 into 3.31):

$$\sigma_w^2 = \sum_{k=1}^{N} \sigma_k^2 \left(\left(\sum_{i=1}^{N} \frac{\phi_i (\phi_i)^\top}{\sigma_i^2} \right)^{-1} \frac{\phi_k}{\sigma_k^2} \right)^2 \tag{3.33}$$

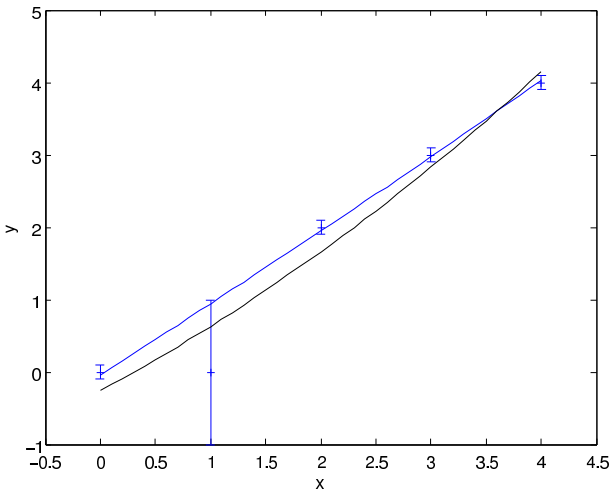

Figure 3.3: *Quadratic fitting example. Black line: standard 2nd order 'polyfit' fit. Blue line: 2nd order polynomial fit using equation above, taking confidence intervals into account. Note the deviation from straight the black line makes, while the blue line doesn't try to fit the second point.*

Using this, the variance of the initial gradient, b, can be given confidence intervals.

It would also be useful to know the confidence intervals for the two points at which the mean current equals zero. One will be approximately at zero, the other will indicate the maximum current flow through the synapse, which when divided by the estimate for the size of the ion channels will find the number of ion channels.

The two points where the parabola meets the x axis can be found using the quadratic equation:

$$x = \frac{-b \pm \sqrt{b^2 - 4ca}}{2c} \tag{3.34}$$

This can be differentiated with respect to y_i, as before with $\mathbf{w}$.

$$\frac{\partial x}{\partial y_i} = -\frac{\left(-b - \sqrt{b^2 - 4ac}\right) a'}{2a^2} + \frac{-b' - \sqrt{-4ca' + 2bb' - 4ac'}}{2a} \tag{3.35}$$

This can be substituted into equation 6, to give the variance. Attempting this the author has found several gradient values to be complex. This is in hindsight to be expected, as some points will not have real solutions, however handling these cases is difficult.

Several alternative options exists:

- The derivative in equation 3.35 could be numerically calculated, this will be slower, but will provide real value results and avoid the complexities of the analytical solution.
- Use the 3 known parameters (a,b and c) and their variances to calculate the variance of this intersection. This will only provide an approximate result, but may be useful.
- Repeat the experiment multiple times, and calculate the variance using the central limit theorem.

The last choice was eventually chosen, as this also isn't affected by the need to assume zero correlation between the parabola's parameters.

3.4.4 Correlation

Equation 3.31 relies on the samples being independent of each other. However, for the charge based analysis, the points on the graph are very closely related, as they are a cumulative measure. Through experimentation this correlation was found to have a very large effect on the estimate of variance of the parabola parameters, and thus heavily underestimated their confidence intervals.

Instead, several charge-variance curves were generated, and a parabola was fitted to each separately. The mean and variance of the parabola parameters were then calculated, and used to find the standard error. This gave much more accurate results for the parameters' confidence intervals.

Chapter 4

Modelling Simple Channels and Cable Filtering

4.1 The Initial Model

4.1.1 NeuronC

NeuronC is a computational modelling tool that allows detailed neural structures to be created and tested *in silico*[19]. The component of most interest for this thesis is the synaptic model. This already includes the markov model and its associated fluctuations that are needed to test the noise analysis.

4.1.2 Current-Based Analysis using AMPA

To test NeuronC, the current-based noise-analysis was repeated to confirm the model produces acceptable results.

Initially this was tried without cable filtering. An AMPA synapse was added to the model and a voltage clamp was applied to the post synaptic segment, clamped at -70 mV. On the presynaptic segment a momentary voltage was applied raising the presynaptic potential to -25 mV. This caused glutamate, a neurotransmitter, to be released, and this caused the ligand gated ion channels to open in the post-synaptic density. The current that then flowed was recorded by the voltage clamp in the post synaptic segment.

The presynaptic impulse was repeated every 100ms, and the resulting current flow recorded. Figure 4.1 shows an example of this recorded current flow (which was usually sampled for at least 10 seconds). The changes in current from single channels opening and closing can be seen, and how the variance in the number of open channels varies with the open probability.

Notice that in the figure the steady state current is in fact about 32pA. This is due to leakage current, and is subtracted to find the current just due to the synapse.

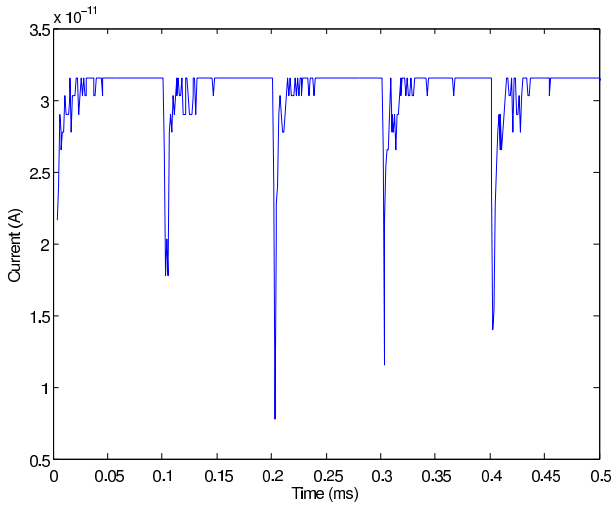

Figure 4.1: *Sample output of NeuronC AMPA synapse with 100 channels.*

The separate iterations were collected and the responses superimposed into a 100ms ensemble. The mean and variance at each time step through that ensemble were then calculated, and plotted against each other.

Figure 4.2 illustrates the mean-variance graph. In this example the initial gradient is found to be -138.9 ± 6.7 fA ($p < 0.05$). The conductance of each channel is 20 pS. There's a 70 mV potential difference across the membrane, so the actual single channel current is -140 fA, within our estimate's confidence intervals.

4.2 The Syn2 Channel

4.2.1 Complexity of the AMPA receptor

The AMPA receptor was considered to be too complicated to try the charge based noise analysis on initially, and so the Syn2 channel type was used instead. Syn2 has just two states, open and closed, with two rates describing the transitions between them (figure 4.3). These rates change during the spike, depending on the amount of neurotransmitter present in the synaptic cleft. Figure 4.4 illustrates this, with the two states in solid red and black.

The charge and variance equations derived in Chapter 3 assumed the channel would be initially open, and that the rates would be constant. This is unfortunately not the case here. However, an equivalent time constant τ_f can be used.

4.2.2 Understanding how τ_f and the rates relate (in the syn2 model)

The opening rate a and closing rate b are related to the transmitter concentration and to the maximum rate $\frac{1}{\tau_f}$. The value of b is the 'opposite' of a, ie: as a moves from 0 to $\frac{1}{\tau_f}$, b moves

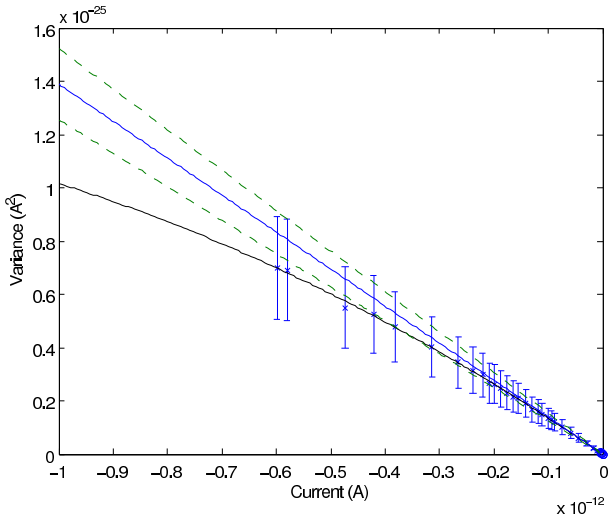

Figure 4.2: *Example of part of the parabola formed by sampling the current and its variance. The curved black solid line is a quadratic fit to the data. The straight solid blue line illustrates the estimate of the initial gradient. The two dashed green lines indicate the 95% confidence intervals of this gradient.*

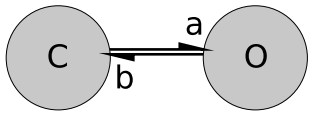

Figure 4.3: *Two states, open and closed. a and b are the rates at which the channel will switch between the two states.*

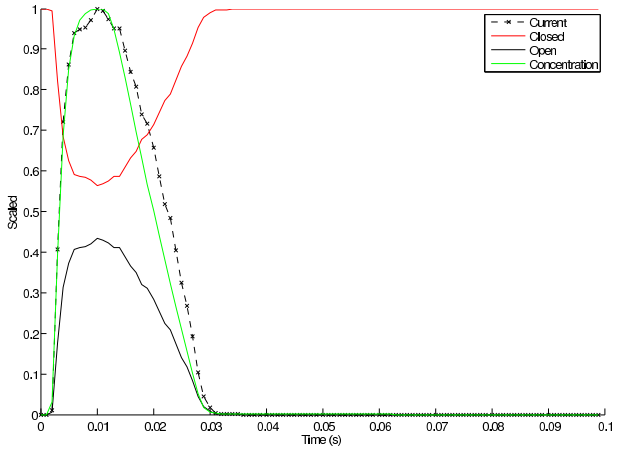

Figure 4.4: *Standard 'syn2' behaviour. Notice the open state closely follows the neurotransmitter concentration. The current and concentration have been scaled to fit between 0 and 1.*

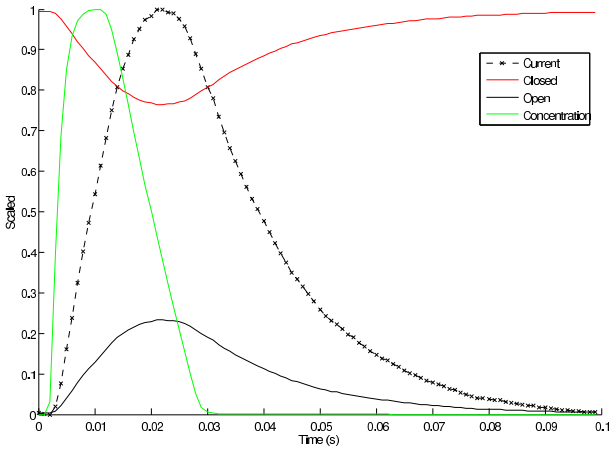

Figure 4.5: *With τ_f set to 100, the decay rate is reduced. The current and concentration have been scaled to fit between 0 and 1.*

from $\frac{1}{\tau_f}$ to 0 [1]. So $a+b=\frac{1}{\tau_f}$. This means that, for a single, steady state channel:

$$p_{open} = \frac{a}{a+b} = \frac{a}{a+(\frac{1}{\tau_f}-b)} = \tau_f a \tag{4.1}$$

and that the time constant for the channel (in any steady state) is:

$$\tau = \frac{1}{a+b} = \tau_f \tag{4.2}$$

To make this more visible, in the time plots, the 'flicker' rate $\frac{1}{\tau_f}$ is decreased (by setting τ_f to 100). This causes the current's decay rate to be slowed (figure 4.5). Although this is biologically unrealistic, it's a useful temporary adjustment that allows the model to be better understood.

We can find the actual rate of decay (ie the rate at which channels go from open to closed) using figure 4.5. Consider two points on the current plot. At time 0.031s there is 80% of the maximum current flowing. At time 0.067s about 11% of current is flowing.

Note that $0.8 \times e^{-2} \approx 0.11$, so the drop from 80% to 11% represents approximately two time constants of exponential decay. As the two samples are 36ms apart, the time constant for the exponential decay is approximately 18ms.

Feeding this into equation 2.32 to find the expected the gradient (remember $i_0 = gv$):

$$gradient = 2\tau i_0 = 2 \times 0.018 \times 20 \times 10^{-12} \times 0.07 = 50.4\text{fC} \tag{4.3}$$

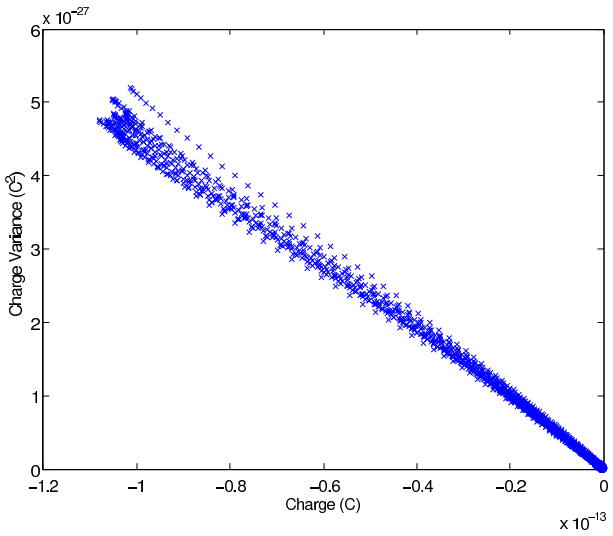

Figure 4.6: *The Charge-Variance graph for the slowed τ_f for the Syn2 channel type.*

4.2.3 Applying the Charge-Based Noise Analysis

Figure 4.6 shows the charge-variance graph for 20 samples. These have an initial gradient of -51.3 ± 1.3 fC ($p<0.05$). The expected gradient is within the confidence intervals, hence this technique appears to work for this simple model.

Section 3.4.4 mentioned the possible problems caused by correlation between sample points, when estimating the gradient's confidence intervals. For the individual gradient samples in figure 4.6, the population variance estimate from the line fitting algorithm is about ± 1.22 fC, while the variance of the 20 samples above is about ± 3.0 fC. The variance is being underestimated by the line fitting because the samples are not independent.

4.2.4 The real decay rate

Why is the decay rate different from the specified rate? For the example above, τ_f is set to be 100ms, but τ is measured to be 18ms.
The temperature of the preparation and other factors will affect this. The Q10 factor describes how various biological processes will change as temperature increases. The `dqsyn` variable was set equal to 1 (instead of its default 3). This should disable the effect of temperature on our model. The experiment was repeated, and in the following analysis the value of τ_f was used to estimate the gradient, and not a measured time constant.

So, τ_f was set to 30ms. The expected gradient calculated using equation 2.32 was -84 fC. The actual initial gradient was -75.8 ± 3.4 fC. The expected gradient slightly overestimated

[1] This relationship was described in an email from Rob Smith, and is defined by the `rsynf` and `rsynr` functions in `chansyn.cc`

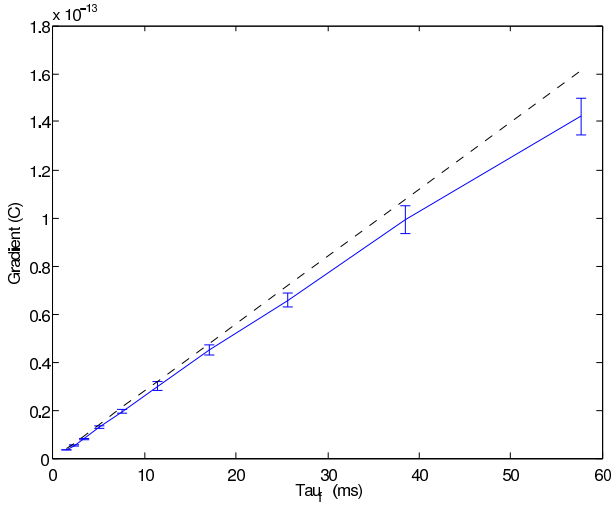

Figure 4.7: *Comparing the expected and actual gradients for different values of τ_f with the synaptic effects of temperature turned off (i.e. the Q10 ratio = 1). Error bars calculated from repeated sampling (95% confidence intervals).*

the actual gradient.

Several gradients and their expected values were plotted (figure 4.7). A general trend of underestimates emerges. There are other features of the cell that are still being affected by the Q10 values, and the pattern of decay in the voltage on the pre-synaptic side may be affecting the gradient also. The model does, however, still provide a good estimate of the charge-variance initial gradient.

4.3 Summary

These results show that the charge-based analysis is possible in theory. It has yet to be seen if the charge-based analysis can be applied to more complex channels, such as the AMPA receptor.

Chapter 5

Applying the Charged Based Analysis to the NeuronC AMPA model

5.1 The Theoretical AMPA Receptor

5.1.1 Kinetic Models

Chapter 4 used the syn2 channel model. The charge-based noise analysis technique was applied to the Syn2 channel, and successfully estimated the initial gradient of the charge-variance graph. This means it is able to predict the single channel conductance. This has so far been for the Syn2 receptor. To be biologically feasible, this must now be extended to the AMPA model.

For the syn2 channel, the simple $O \rightarrow C$ model was used. It has been shown that the initial gradient of the Charge-Variance graph for that model is equal to:

$$2i_0\tau \tag{5.1}$$

Where τ is the time constant of the closing rate.

It is now necessary to consider the more complex AMPA receptor. The NeuronC model has this receptor already defined. There are several kinetic models of this receptor, some with more than one open state. One example (used during the *Neural Computation* course) can be found in Destexhe, Mainen and Sejnowski[2, p8] (figure 5.1).

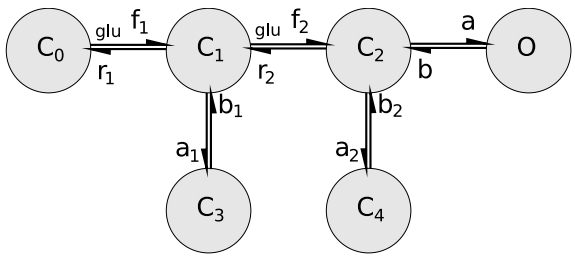

Figure 5.1: *The AMPA kinetic model from Destexhe, Mainen and Sejnowski[2].*

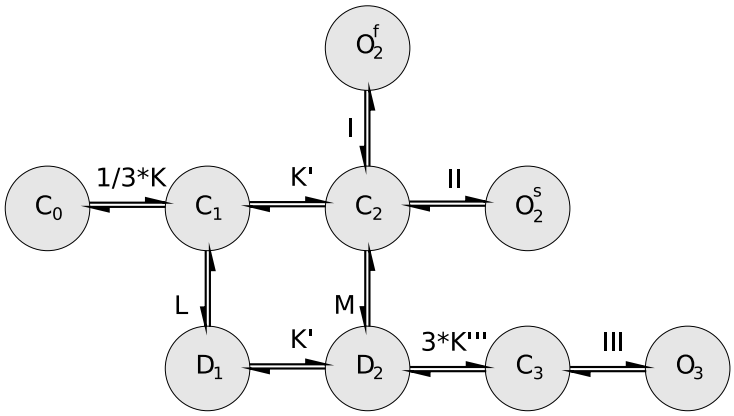

Figure 5.2: *The AMPA kinetic model from Raman and Trussell[15]. Note this model has three open states.*

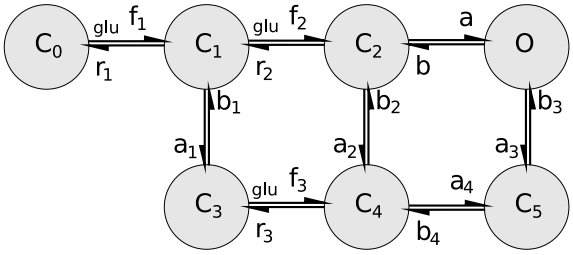

Figure 5.3: *The AMPA state model used by the NeuronC modelling software (described as Type 1 in the documentation).*

Almost arbitrary levels of complexity can be added to these models, to improve their fit with experimental data. For instance, Raman and Trussell's 1995 paper[15, p143] describes in 'scheme 2' a kinetic model with three open states (figure 5.2).

The NeuronC software uses Jonas et al's[8, pp 655-656] AMPA receptor (figure 5.3). This is similar to Destexhe's but with another deactivated state (C_3), and includes transitions between the deactivated states.

States C_0, C_1 and C_2 are the unbound, partially bound and fully bound states, respectively. C_3, C_4 and C_5 are the deactivated states.

5.1.2 Simplifying the Model

To simplify the problem initially, the a_1, a_2 and a_3 rates were reduced to zero. This leaves out the deactivated states, leaving just C_0, C_1, C_2 and O.

The initial gradient will be formed by the behaviour of the synapse at very low open probabilities. Most of the time the synapse is active, its response is 'decaying' as the neurotransmitter gradually reduces (figure 5.4). So most of the low open probability will be when the concentration is low, and the channels will not be entering C_2 from C_1.

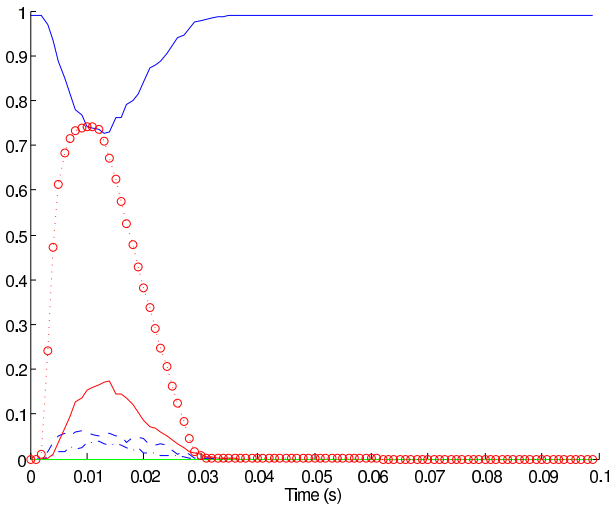

Figure 5.4: *Behaviour of the simplified AMPA receptor. The blue lines are: C_0 solid, C_1 dashed, C_2 dash-dotted. The solid red line is the open state. The circle-marked line indicates the neurotransmitter concentration in the synaptic cleft.*

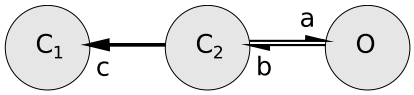

Figure 5.5: *The three states of interest during decay (note the r_2 rate has been relabelled c).*

Therefore, the variance in the number of channels in the open state will depend largely on the rate to and from it, and from C_2 to C_1 (figure 5.5).

This is ideal, as the transition rates no longer depend on the neurotransmitter concentration.

5.1.3 Computing the Initial Gradient

This state diagram can be converted into a Markov Matrix, and the mathematical technique outlined in Chapter 3 can be applied to predict the charge and charge variance of the ion channel.

As described earlier, the charge is calculated by integrating from a time, t_0, to infinity. The equation for the charge-variance gradient is quite complex, but as $t_0 \to \infty$, the resulting initial gradient can be simplified, and is found to be:

$$gradient = \frac{2(a+c)}{bc} i_0 \tag{5.2}$$

This can also be found using the following logic:

First, considering a single channel with one open state in which $i_0 = 1$: The charge-variance graph will be a parabola (proved in section 3.2.2). The peak of the parabola occurs where $t = 0$. It is known that this occurs at the point where:

$$charge = \frac{a+c}{bc}$$

and

$$variance = \frac{(a+c)^2}{(bc)^2}$$

For any parabola the initial gradient (at $x = 0$) is twice the gradient of a straight line from the point at $x = 0$ to the peak. In this case the gradient will be:

$$2 \times \left(\frac{\frac{(a+c)^2}{(bc)^2}}{\frac{a+c}{bc}} \right)$$

which equals expression 5.2 for gradient above (if $i_0 = 1$).

5.2 Comparison with model results

5.2.1 Transition Rates

The AMPA model in NeuronC had the deactivation transitions disabled, by setting `tauc = 1000` and `taud = 1000`. This meant the deactivation (and reactivation) rates were reduced to approximately zero.

The three transition rates of interest are now a, b and r_2 (rewritten c). By default these rates are:

- $a = 4240s^{-1}$
- $b = 900s^{-1}$
- $c = 3260s^{-1}$

5.2.2 Results

These values for a, b and c were each altered, to test equation 5.2 using the AMPA model described.

Figures 5.6, 5.7 and 5.8 show how the gradient changes as these rates are altered, and how these match the theoretical prediction. The three graphs suggest the prediction using the analysis from chapter 3 closely matches the model results.

It appears however, in figure 5.7 that the gradient is not successfully predicted for low b rates. This would correspond to the channels closing slowly (as b is the transition from from Open to Closed).

5.2.3 Integration Time

Figure 5.9 shows how the states change over time (for $b = 40s^{-1}$). This shows that the channel is not yet closed at the end of the integration period. This will both affect the Open $\rightarrow$ Closed

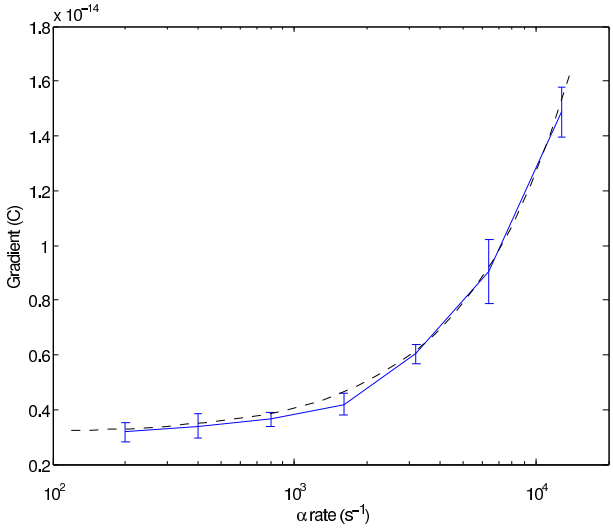

Figure 5.6: *Expected and actual gradients as the a rate constant changes (black dashed line is the theoretical value, and the blue line is the measured value).*

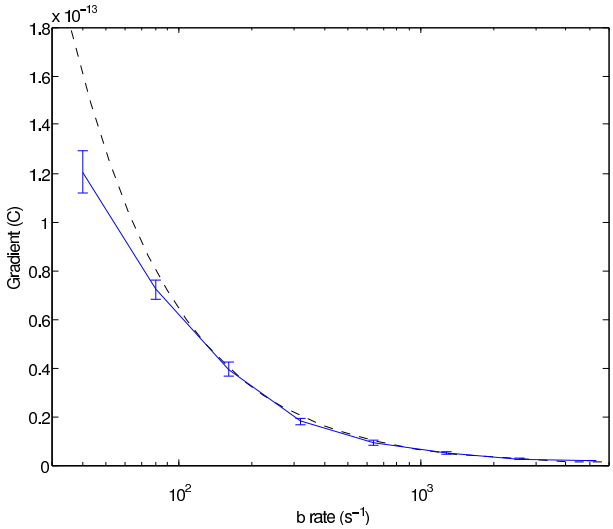

Figure 5.7: *Expected and actual gradients as the b rate constant changes (black dashed line is the theoretical value, and the blue line is the measured value).*

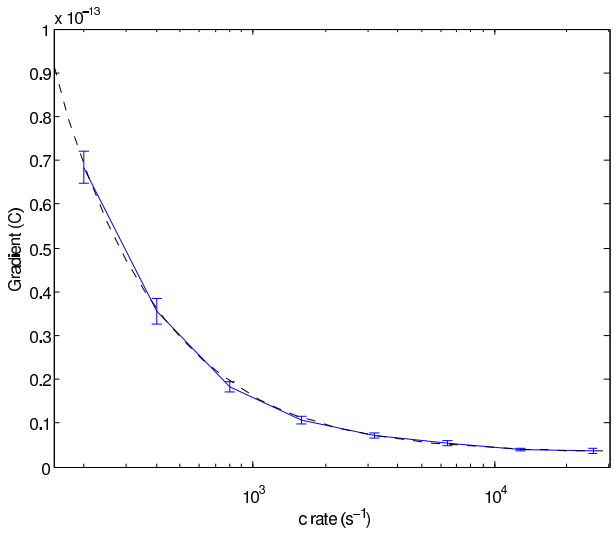

Figure 5.8: *Expected and actual gradients as the c rate constant changes (black dashed line is the theoretical value, and the blue line is the measured value).*

analytical solution and the behaviour of the channel (as it will still be open when the next presynaptic impulse occurs). This explains the error in gradient. To avoid this error it is important to make the integration period long enough. This however means the simulation produces fewer samples, widening the confidence intervals.

5.3 The Full AMPA receptor

5.3.1 Results

For the simplified model (without deactivated states), by using the transition rates (a, b and c) the initial gradient can be estimated for a particular single channel current, i_0. Or, given an experimentally discovered initial charge-variance gradient, i_0 can be calculated.

This is true of the simplified model, but what of the full AMPA receptor? The deactivated states were added again (by setting a_1, a_2 and a_3 back to their default values). The estimate of i_0 using this technique gives $i_0 = 1.34 \pm 0.12pA$ (p<0.05), the expected current is $1.4pA$, so the model successfully predicts this current.

5.3.2 Why does the technique still work?

The addition of the deactivated states should have altered the channel's kinetics, causing the prediction to fail. However, some of the transition rates into the deactivated states are already small (figure 5.10). Specifically the transitions from the Open state (O) and the fully-bound Closed state (C_2). These are small enough to have little effect on the overall kinetics. For example the transition from C_2 to C_4 is only 2.2% of all the transitions from C_2.

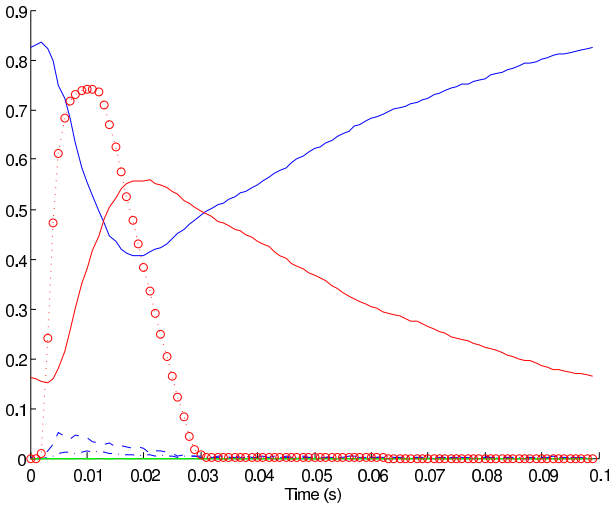

Figure 5.9: *Behaviour of ion channel for a low b rate. The solid red line is the open state, the blue lines are the closed states (solid - unbound, dashed - partially bound, dash-dotted - fully bound). The green line at zero are the deactivated states, and the line marked with circles indicates the neurotransmitter concentration in the synaptic cleft.*

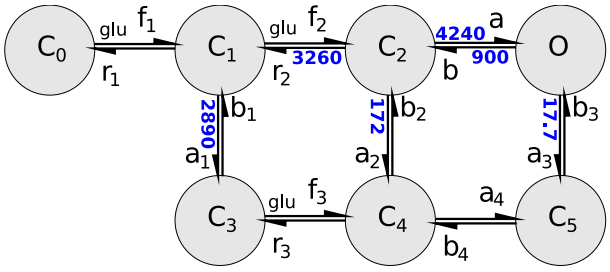

Figure 5.10: *The actual rates for the AMPA transitions of most interest. The rates are in s^{-1}. The full list of transitions are listed in appendix A.*

Chapter 6

Cable Filtering with Syn2

6.1 Introduction

In chapters 4 and 5 the microelectrode was at the synapse, this meant there was almost no measurable cable filtering. In this chapter and the next, a length of dendrite has been added to the model to simulate a distal synapse. A couple of configurations are tested, to see how the estimates of the single channel conductance change with cable filtering.

6.2 Building the Cable

As mentioned in section 1.2, cable filtering causes the current based noise analysis to underestimate the single channel conductance. To simulate cable filtering in NeuronC, the dendrite and soma of the cell were modelled using multiple compartments.

These compartments had to be small enough to avoid numerical inaccuracies, but large enough to make the simulation run reasonably quickly. A length of $\frac{1}{20}$th the space constant was suggested for the *Neural Computation* coursework, and is the value used here.

This means that the number of segments, n:

$$n > \frac{20l}{\lambda} \tag{6.1}$$

where l is the length of the cable and λ is the space constant, which can be found using:

$$\lambda = \sqrt{\frac{dr_m}{4r_i}} \tag{6.2}$$

In this case:

$d = 1\mu m = 1 \times 10^{-6} m$

$r_m = 40,000 \Omega cm^2 = 4 \Omega m^2$

$r_i = 200 \Omega cm = 2 \Omega m$

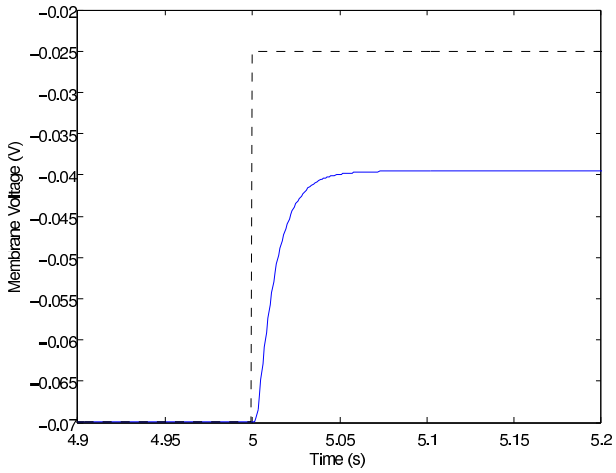

Figure 6.1: *Effect of cable filtering. A voltage clamp is applied after 5s to one end of the dendrite. The black dashed line indicates the membrane voltage at this point. 700 µm from this point the voltage is also recorded (blue solid line), which is approximately one space constant from the clamp. This voltage is 67.7% of the input voltage.*

So the space constant is:

$$\lambda = \sqrt{\frac{10^{-6} \times 4}{4 \times 2}} = 707 \mu m$$

So, for a given length (in μm):

$$n > \frac{l}{35.35} \tag{6.3}$$

6.3 Checking the space constant and model

The space constant was checked using the model. Figure 6.1 shows an example comparison, but this finds the space constant equal to:

$$\lambda = \frac{-700}{ln(0.67)} = 1,791 \mu m$$

considerably more than expected. The cable was made 7000 μm long, and the experiment repeated, but with the sampling half way along the cable, to reduce 'end effects'. In this case, the recorded signal was only 0.69% of the input voltage.

$$\lambda = \frac{-3500}{ln(0.0069)} = 703.6 \mu m$$

Almost exactly the expected value.

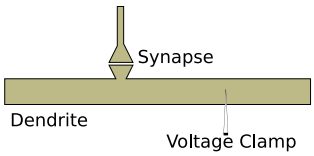

(a) Infinite cable

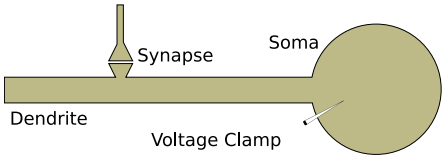

(b) 'realistic' location, partway along a dendrite

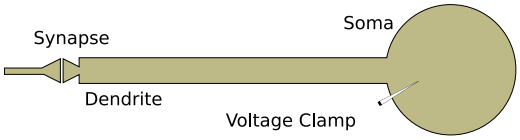

(c) At end of a dendrite

Figure 6.2: *Possible synapse locations to test*

6.4 Configurations of Cable

As mentioned in chapter 1, the estimates of channel parameters are seriously distorted by the introduction of cable filtering. To model cable filtering, several possible configurations of synapse need to be considered (figure 6.2).

6.4.1 'End-of-dendrite' Model

First the 'end-of-dendrite' model (figure 6.2(c)), using the syn2 synaptic states, was tested. Using $\tau_f = 30ms$ the estimate of i_0 was sampled as the cable length increased (figure 6.3). This shows a decline in the estimate as the cable length increases, both for the current-based analysis and charge-based analysis.

Examining figure 6.3, it appears the charge-based estimate has two unexpected features. First, it doesn't appear to be correct at zero cable length, but slightly underestimates the single channel current. Second, because the effect of cable filtering is cumulative, the curve might be expected to decay exponentially - this hypothesis is substantiated later, using the cable equation. This does require many assumptions (for example an infinite cable). Note that the estimate appears to decay slowly initially; Not an exponential decay.

Possible causes for these two oddities include:

- The large soma
- Voltage fluctuations at synapse

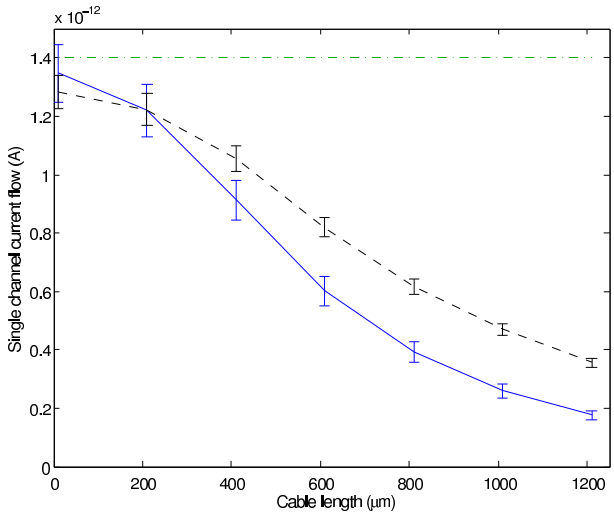

Figure 6.3: *The estimates for the single syn2 channel current for different cable lengths using the 'end-of-dendrite' model (figure 6.2c). The synaptic effects of temperature are disabled. Error bars calculated from repeated sampling (95% confidence intervals,* $\tau_f = 30ms$*). The blue solid line is the current-based estimate, the black dashed line is the charge-based estimate and the green dash-dot line is the approximate actual value.*

- Some temperature dependent features of the model still enabled
- Kinetics of channels not just Open → Closed.
- Poorly seeded experiment (each point calculated with same seed)

Reducing the size of the soma (from 100 μm to 2 μm) had no effect. Possibly the voltage at the synapse wasn't at 0.07V as used to estimate the actual current flow. Figure 6.4 shows the voltage at the synapse. Although it does appear to vary slightly, it does not appear to be enough to explain either of the effects mentioned above.

6.5 Synapse partway along cable

Various lengths of extra cable were added to the synapse's end, extending the cable, to investigate the cable's 'end-effect'. Figure 6.5 illustrates how this reduces the estimate of i_0. This is probably because the extra cable acts like a capacitor, filtering higher frequencies, thus hiding the variance and reducing the end effect (allowing more of the current to flow into the 'extra' cable). The end-effect may explain the oddly delayed decay at small cable lengths.

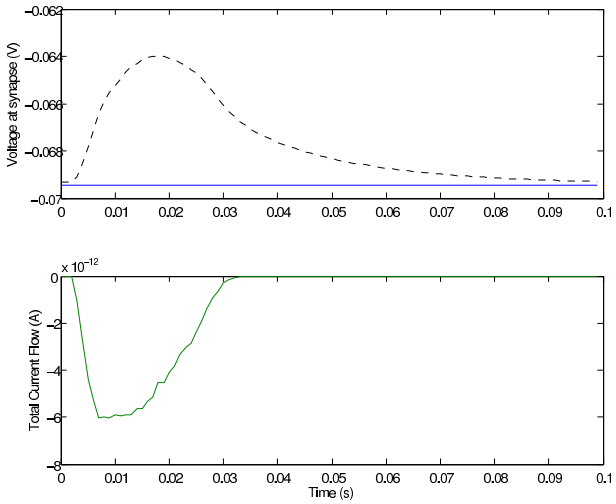

Figure 6.4: *How the voltage at the synapse changes as the channels open. The black dashed line is for when the soma is 1.2 mm from the synapse, and the blue solid line for when there is no distance. The lower graph is to illustrate when the channels open, and describes the current flow through the synapse. 10 channels were used in this simulation.*

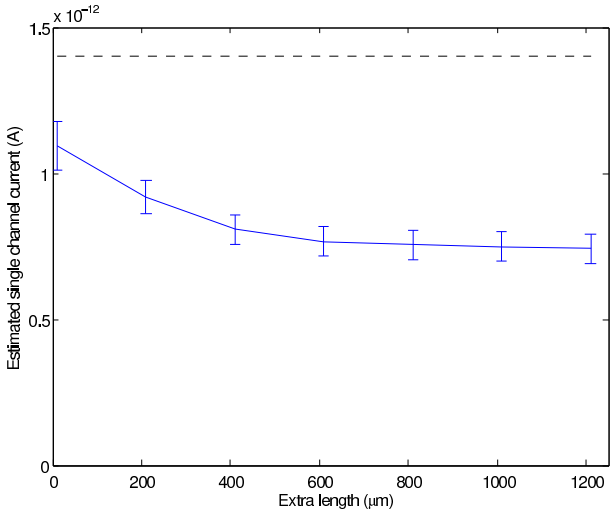

Figure 6.5: *Effect of extra cable on prediction for the single channel current (using the charge-based noise analysis). Note the synapse is 350 µm from the soma, hence the underestimate at 0 µm of extra cable. The black dashed line is the approximate actual value.*

Chapter 7

Cable Filtering with AMPA

7.1 Understanding Cable Filtering

7.1.1 Creating a Suitable Model

Cable filtering can be added to the AMPA model, by placing a dendrite between the Soma and the synapse, as in figure 6.2(c). As for the syn2 channel, the single channel current is underestimated for longer cables. These estimates are illustrated in figure 7.1 as the black dashed line.

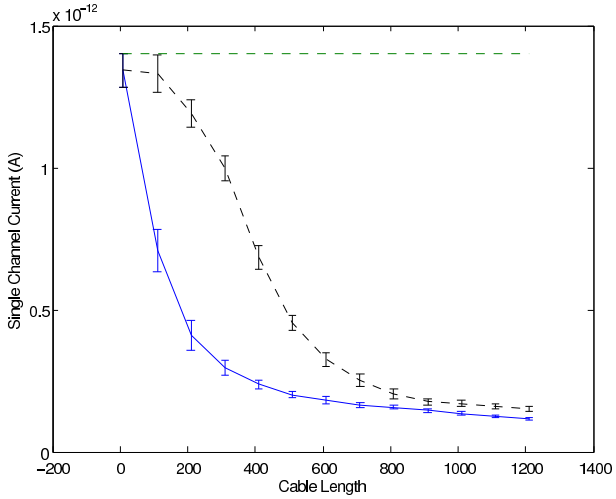

Figure 7.1: *The estimate of the single channel current drops off more quickly when there's extra cable (blue solid line), so the synapse is not near the end of the dendrite. This is more realistic than the synapse-at-the-end (black dashed line) model. The extra length of cable was fixed at 700 µm.*

As was noted in section 6.5, the end-effect caused by placing the synapse at the end of the cable stops the curve decaying exponentially. By adding 700 μm of dendrite beyond the synapse, the end effect can be removed, and the curve begins to appear far more like an exponential decay (figure 7.1).

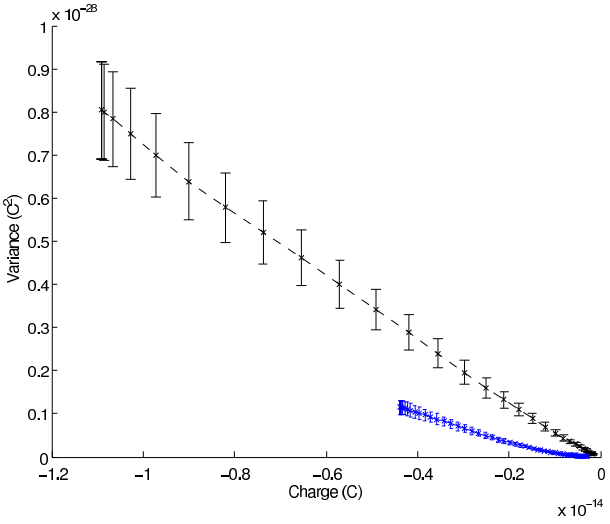

Figure 7.2: *Effect of one space-constant's worth of cable filtering on the size of the Charge-Variance graph. The solid blue line is for 700 µm from the synapse. The dashed black line is without filtering. The extra length of cable was fixed at 7000 µm.*

7.1.2 Steady State Membrane Leak

The next step is to discover what is causing the underestimate of the channel current. The current flowing from the synapse to the soma can also flow out of the dendrite, through the membrane, causing less charge to reach the soma. A steady state flow will only be lost via the conductance of the membrane, while the capacitive effect of the membrane will cause the transient component of the input current to escape. The effect of this filtering can be simplified by assuming that just the *steady state* loss is important.

The full cable equation is:

$$c_m \frac{dV_m(x,t)}{dt} = \frac{d}{4r_i}\frac{d^2V_m(x,t)}{dx^2} - \frac{1}{r_m}V_m(x,t) + I_{ext}(x,t) \tag{7.1}$$

Where, c_m is the membrane unit capacitance, d is the diameter of the dendrite, r_i is the axial or intracellular resistivity and r_m is the membrane resistivity. The membrane voltage, V_m and injected current I_{ext}, are dependent on the position along the dendrite, x, and the time, t.

The injected current is, in the steady state model, continuous. It is placed at $x = 0$, and is written as $I_0\delta(x)$. This expression describes an infinite spike of current at $x = 0$, but with an integral over x equal to I_0. In this steady state, the time component can be removed, and the derivative with respect to time set equal zero. Multiplying through by r_m, leaves:

$$-r_m I_{ext}(x) = \frac{dr_m}{4r_i}\frac{d^2V_m(x)}{dx^2} - V_m(x) \tag{7.2}$$

The space constant λ is:

$$\lambda = \sqrt{\frac{dr_m}{4r_i}} \tag{7.3}$$

So the differential equation's characteristic equation can be written:

$$0 = \lambda^2\phi^2 - 1 \tag{7.4}$$

Which means the eigenvalues are, $\phi = \pm\frac{1}{\lambda}$. This equation therefore has solution:

$$V_m(x) = a_0 e^{-x/\lambda} + b_0 e^{x/\lambda} \tag{7.5}$$

The constants, a_0 and b_0 can be found by considering particular locations on the cable based on assumptions about its geometry. If it is assumed that the cable stretches from $x = 0$ to infinity, then one may consider how the membrane voltage, $V_m(x)$ changes as $x \to \infty$. The voltage must remain finite. For this to be possible, $b_0 = 0$, to avoid the exponential increase. This leaves:

$$V_m(x) = a_0 e^{-x/\lambda} \tag{7.6}$$

At $x = 0$, $V_m(0) = a_0$. In this case the voltage is that caused by the current through the ion channels in the synapse. For the purpose of this analysis, the exact value does not matter. Instead, focus on the exponential decay shown to exist along the length of the dendrite. The voltage drop along a cable, in the steady state case is, therefore:

$$V_{out} = V_{in} e^{-l/\lambda} \tag{7.7}$$

Where V_{in} and V_{out} are the input and output voltages. λ is the space-constant while l is the distance to the synapse from the microelectrode (at the soma). So $\frac{l}{\lambda}$ is the electrotonic length. The current flowing into the soma will also decay by the same rate, as the current is proportional to the voltage (in this steady state example).

Note that during the analysis above, it was assumed the cable was infinite. The decay will be different with a finite length of dendrite.

7.1.3 Effect on the Charge and Variance

The charge will be affected in the same way, as it is the integral of the current over time. Therefore, the amount of charge getting to the soma will also be proportional to $e^{-l/\lambda}$. This can be observed in the reduction in the width of the charge-variance graph (figure 7.2). The peak of the unfiltered graph has a charge of 11fC, while the filtered peak has a charge of only about 4.3fC. The expected ratio is $e^{-1} \approx 0.36$, which is approximately the ratio between the two peaks.

For a random variable X,

$$Var(aX) = a^2 Var(X) \tag{7.8}$$

In this case the charge is the random variable. We know the charge has been scaled by $e^{-l/\lambda}$, so the variance will be scaled by $\left(e^{-l/\lambda}\right)^2$. The gradient of the variance/charge graph

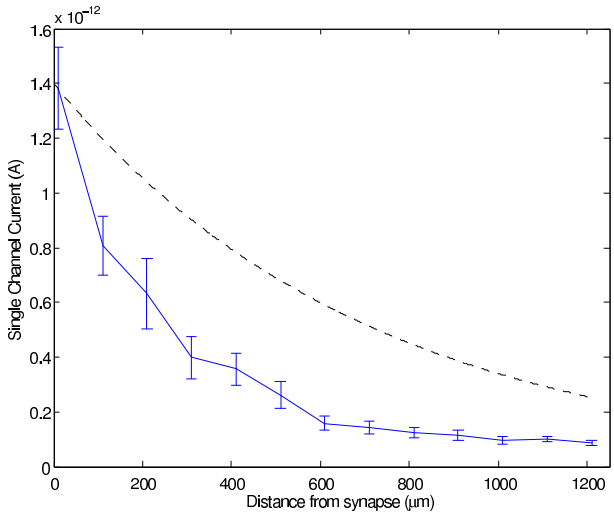

Figure 7.3: *Comparing the decay of the charge-based estimate of i_0 with the expected decay due to steady-state cable filtering. The solid blue line is the estimate of i_0, the dashed black line is the expected decay. The extra length of cable was fixed at 7000 µm.*

will therefore be scaled by,

$$\frac{\left(e^{-l/\lambda}\right)^2}{e^{-l/\lambda}} = e^{-l/\lambda} \tag{7.9}$$

As the estimate of i_0 is proportional to the gradient, one might expect the i_0 graph to decay at this rate. This hypothesis is tested by plotting the exponential curve $e^{-l/\lambda}$ on the same graph as the estimate of i_0 (figure 7.3). The measured curve seems to decay initially much faster, before levelling off. This is a poor fit and so there must be more filtering to be accounted for.

7.2 Improved Estimate

7.2.1 Measuring the Gradient

To discover the cause of the distortion, it is worth examining the charge-variance plots being created by the cable filtered model. The calculations use the initial gradient of the curve to estimate the single channel current. A parabola, fitted to the curve, is used to find the initial gradient. Figure 7.4 shows that this initial gradient is heavily affected by the cable filtering, as the curve is no longer parabolic (especially at small values of charge).

Cable filtering doesn't appear to affect the charge peak as much as the bottom of the curve. The total charge that flows to the soma will be affected less than the charge over shorter periods of time. This is central to the original concept of using charge, rather than current, in the analysis.

So instead of taking the gradient at zero charge, a line from zero to the peak can be drawn, and the gradient of this used instead (see figure 7.4). This will only work if a relatively small number of channels open. In the simulation usually only 10%-20% of channels open in the

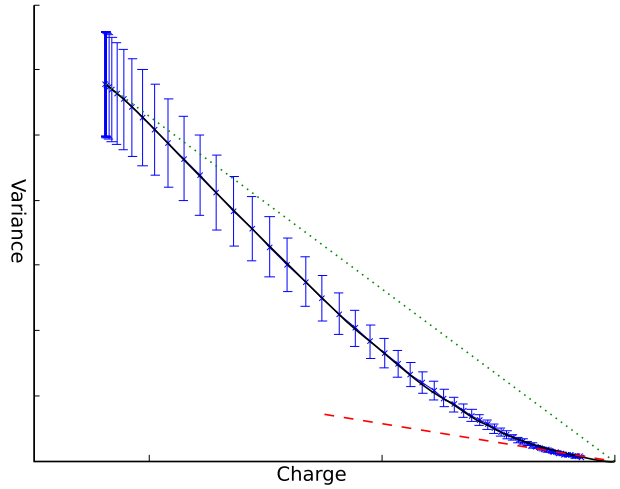

Figure 7.4: *The black curve is the shape of the Charge-Variance graph, due to 700 µm (one space constant) of dendrite. In dashed red is the original gradient measure. In dotted green is the potential new way of measuring the initial gradient.*

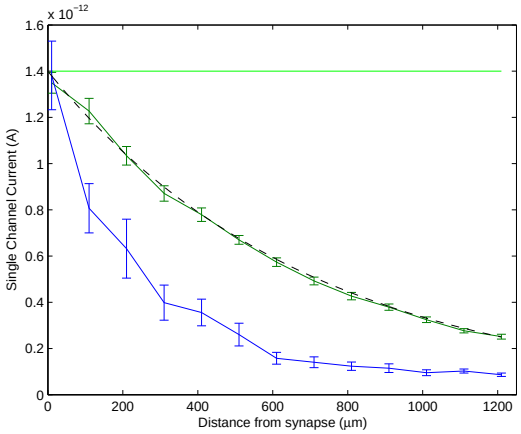

Figure 7.5: *The larger gradient (solid green line) is much closer to the expected exponential decay (black dashed line) than the original gradient (solid blue line). The horizontal green solid line indicates the actual single channel current.*

AMPA model used. If many open, then a point must be picked on the curve, to compromise between the cable filtering effect at the bottom, and the parabolic curvature at the top. If enough of the parabola is plotted, then the initial gradient could be calculated using curve fitting on the paraboic portion.

Figure 7.5 illustrates the estimates using the larger gradient (green solid line). The decay in the estimated channel current is much closer to the exponential decay expected (black dashed line), than the original gradient estimate.

7.2.2 Correcting for the cable filtering

By dividing the gradient by the expected steady-state decay, a corrected estimate for the single channel current i_0 can be found. This is plotted in dashed blue in figure 7.6. As can be seen, this seems to provide a solid estimate of i_0.

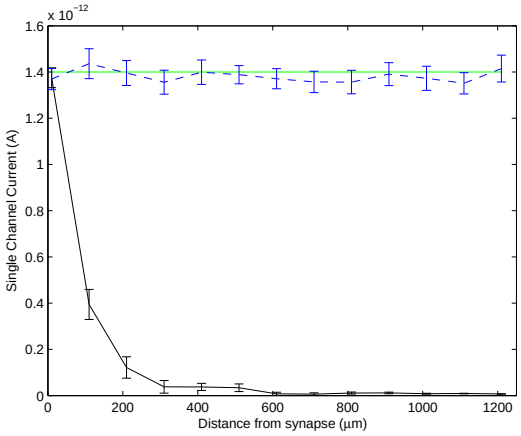

Figure 7.6: *The black solid line is the current-based estimate of i_0. The blue dashed line is the estimate using the 'zero-to-peak' gradient, divided by $e^{-l/\lambda}$, correcting for the steady-state cable filter. The green solid line is approximately the actual value of i_0.*

7.3 Estimation Accuracy

7.3.1 Description

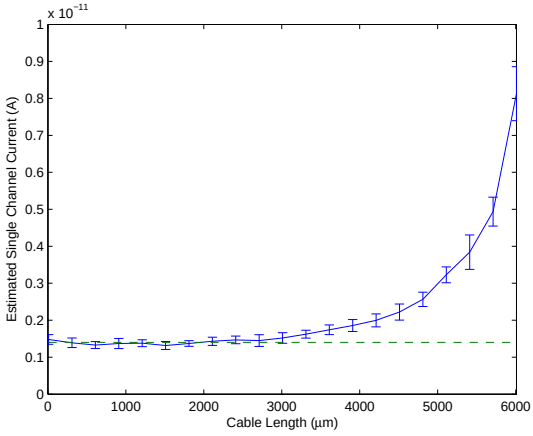

Figure 7.7: *The solid blue line is the estimate of i_0. The green dashed line is the actual value of i_0. $\lambda = 700\mu m$, so the estimate begins to fail with a cable of 4 or 5 λ. The error bars are 95% confidence intervals.*

The charge-based technique, using the 'zero-to-peak' gradient estimate, appears to provide a very good estimate for medium lengths of cable, with the actual value being within the 95%

confidence intervals of the estimate. If longer cables are considered, eventually the estimate begins to fail. Figure 7.7 shows how the technique begins to overestimate the actual current. It appears to fail when the cable is more than about 4λ. This may not seem very long, but synapses are generally within 2λ of the soma[6]. Also note that at 4λ, the current at the soma will be less than 2% that at the synapse. It is likely that with this small current (probably only a few femtoamps), the error due to thermal noise and distortion will undermine the analysis anyway.

7.3.2 Different Numbers of Channels

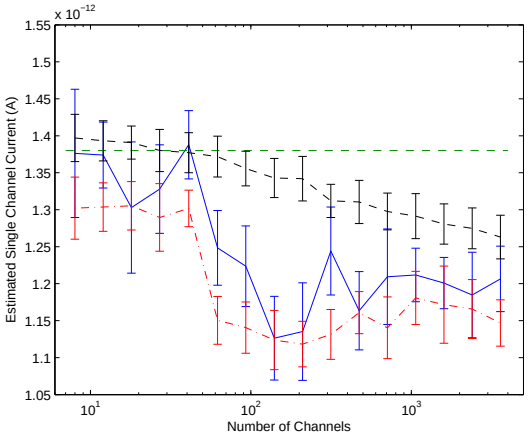

Figure 7.8: *Affect on the estimate of single channel current as the number of channels changes, without cable filtering. The blue solid line is the charge-based analysis using the 'zero-to-peak' gradient. The red dash-dotted line is the current-based analysis using the 'zero-to-peak' gradient also. The black dashed line is the current-based analysis using the original parabolic fit.*

It was assumed earlier that the number of channels didn't affect the initial gradient. To speed up the simulations, just 10 channels were simulated. It appears however that the gradient falls as more channels are modelled. Figure 7.8 illustrates this.

The most obvious possible cause of the underestimate is that the extra current flow causes the voltage at the synapse to drop. The voltage at the synapse was recorded, but appeared not to fall, even with many more synapses opening. The current-based analysis was applied, and appeared to fall in a similar way to the charge-based analysis. Using the parabolic fit to find the initial gradient instead appears to be a better fit, but also begins to decay as more channels are added.

If the effect was caused by the voltage falling, the estimate would be expected to decay as the number of channels increased. However, it appears to level out above about 100 channels. It may be the voltage at the synapse itself is falling, and the voltage NeuronC is recording is not quite the same. Or alternatively NeuronC may be modelling the effect more channels have

on the distribution of neurotransmitter, or the voltage outside the synapse.

Qualitatively, during experimentation and while examining the charge-variance curves, it appears the curves are more likely to curve into parabolas when more channels are available. This isn't expected, but could explain the drop in gradient, as the gradient is currently calculated as that of a straight line drawn from the bottom to the top of the curve. This hypothesis is supported by the estimate using the parabolic fit. The black dashed line in figure 7.8 uses the parabolic fit to find the initial gradient. It seems to avoid the sudden underestimate at about 50 channels. However, it does still seem to fall slowly. The underestimate may therefore be caused by two separate effects.

The cause of these estimation errors is unclear, but may be due to approximations within the NeuronC model. Further experimentation is required to understand them.

Chapter 8

Analysis and Improvements

8.1 Results

The charge-based technique with corrections for cable filtering was able to predict the single channel conductance of a distal synapse. It was shown that other features of the synapse, such as the number of channels, may be found using the technique. The new method is an improvement upon the current-based analysis for distal synapses, with known kinetics.

The charge-based noise analysis does have several shortcomings, listed below. Many of these are potentially soluble, with further work.

8.2 Data Required

The charge based technique's main flaw is the amount of data it requires. Besides an accurate microelectrode recording, the electrotonic distance to the synapse is required, and knowledge of its state-kinetics. These may be known in advance, but the electotonic distance will either need to be inferred from the shape of the recorded spike, or possibly discovered by examining the histology of the sample[16].

8.3 Channel types

It is assumed that the channel's transition matrix is known, and so the technique in chapter 3 can be used to find the charge-variance relationship for a single channel, thus allowing the size and number of channels to be calculated. However, it is known that AMPA receptors are not identical. An AMPA receptor is constructed from four subunits (two GluR2s and two others). The GluR2 subunit can be modified in several ways. For instance, post-transcriptional RNA editing the Q/R site of GluR2[9] alters the channel's calcium conductance. Another example due to splicing variants causes changes in the flip/flop region of the protein. These change the

channel's desensitisation kinetics[12].

These variations may distort the results, unless the specific AMPA variant has been identified. However, if several different variants are present this may be impossible.

8.4 Gradient Estimate

In section 7.2.1, it was suggested that the peak of the curve should be used, rather than the initial gradient. This would work for low ratios of channels opening. However, if channels opened with larger probabilities then the curve would begin to enter the parabola.

Two possible ways of finding the initial gradient become available as the curve is extended. Either a point on the curve can be chosen that is not affected by cable filtering but is also not affected by the parabola. Alternatively a subset of the curve, that is least affected by cable filtering, can be chosen, and used to extrapolate the gradient at the origin.

The former method was tried, but the data was found to be too noisy to reliably find the point of maximum gradient, which might indicate the balance between the cable filtering and the parabola. Smoothing was applied to avoid this noise, but the technique seemed fraught with arbitrary factors, such as the type and size of smoothing.

The latter technique still requires a point to be chosen that marks the end of the cable filtering, but has potentially better noise immunity.

8.5 Noise

8.5.1 Sources of Noise

In this model, no external noise was considered. All the fluctuation in the data came from the channels opening and closing. Real data will have noise from many sources. Example include thermal noise in the cell and the electronic equipment, other channels, variations in vesicle sizes and changes in the synapse over time.

8.5.2 Modelling the noise

Although the noise could take on many forms, including forms of distortion, it was decided that additive Gaussian noise would be most easily applied and understood.

8.5.3 Effect on estimates

The size of the noise is defined by its standard deviation, as a percentage of the peak flow possible through the synapse. So with $N = 10$ and $i_0 = 1.4$pA, the noise is a percentage of 14pA (the peak current flow possible).

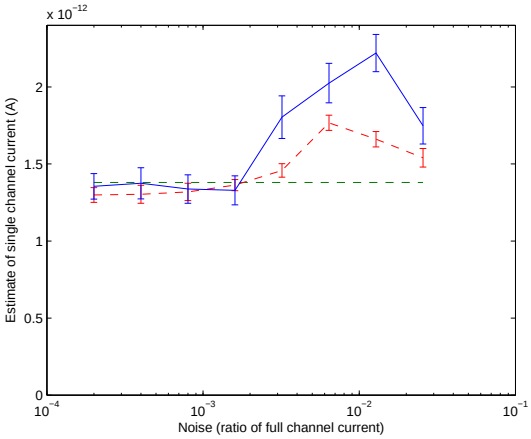

Figure 8.1: *Effect of additive gaussian white noise to the estimate of single channel current. The solid blue line is the estimate for the charge-based analysis. The red dashed line is for the current based analysis.*

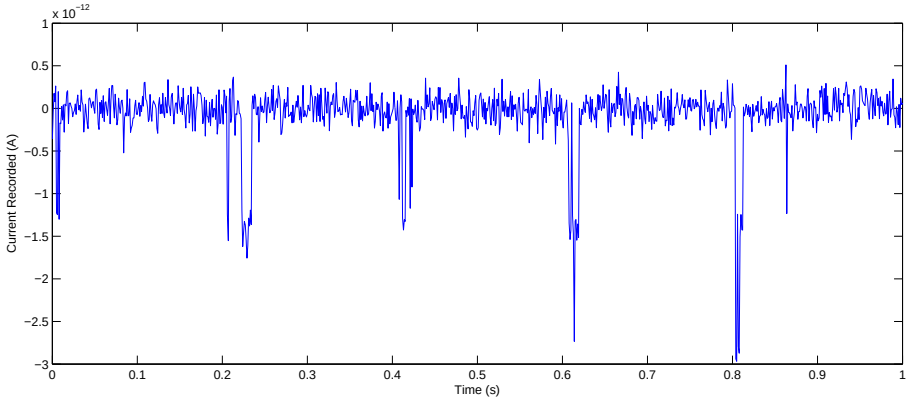

Figure 8.2: *Sample of recorded data, with additive 140fA s.d. white gaussian noise.*

The charge based estimate is accurate until the standard deviation of the noise reaches about 0.2% (28fA). Both the charge and current based estimates seem to be affected by the noise in a similar way. With overestimates becoming more likely as the noise increases. Figure 8.2 illustrates what noise with a standard deviation of 140fA (1%) looks like. Clearly the original signal is harder to analyse, especially the decay after the peaks.

8.6 Estimating the Number of Channels

8.6.1 Using the parabola

In chapter 7 the single channel current i_0 was found. It is also interesting to know the number of channels, N, in the synapse. So far the analysis has focused on using the initial gradient of the parabola. This doesn't depend on the number of channels, N, so other features of the curve must be used.

The peak of the parabola is one such point. If all the channels are initially open before they decay, then, using the same markov matrix that was used in section 5.1.3, the peak of the parabola is found to be where:

$$charge = \frac{2a+b-2c}{ab-bc} \tag{8.1}$$

and

$$variance = \frac{4a^4+a^3(2b-16c)+ac(-2b^2+6bc-16c^2)+c^2(b^2-2bc+4c^2)+a^2(b^2-4bc+24c^2)}{b^2(a-c)^2(a-2ac+c^2)} \tag{8.2}$$

The equation for peak charge is used in the following analysis, as it is far simpler than that for variance.

8.6.2 Finding the peak

The majority of charge-variance curves produced during this report have been of the approximately straight initial part of the parabola, and the parabolic nature of the curve was difficult to see. Indeed for smaller values, the line curved the wrong way (due to the cable filtering).

In all the examples so far, only a few of the channels were open. Figure 5.4 shows a maximum of 20% of the channels open. This means most of the parabola is hidden and only a small proportion is shown (which appears straight). Still using the AMPA model, but with no cable filtering, the presynaptic pulse was increased from -0.025mV to +0.25mV. This allowed the start of the parabolic curve to become visible, and the position of the peak to be extrapolated, as in figure 8.3. The increased input voltage did cause a slight cable-filtering like change to the parabola, even though the signal was not cable filtered. This meant it still appeared to curve incorrectly at low values. To avoid this, only values above 10% of the mean variance were used in calculating the quadratic fit. The cause of the slight curve is not fully understood, but at higher voltages, the assumptions regarding the channel kinetics weaken as more channels enter the inactivated state. This may be due to the higher concentration of neurotransmitter.

8.6.3 Confidence

Figure 8.4 shows the variability in the estimates for the peaks, and the problem when trying to estimate the peak. Eventually 569 curves were sampled, each using 5000 spike recordings to compute the mean and variance. The position of the peak was estimated to be at 476 ± 12 fC.

By expanding equation 8.1 for the total charge, Q_T, for N channels with single channel current, i_0, it can be shown that:

$$Q_T = N i_0 \frac{2a+b-2c}{ab-bc} \tag{8.3}$$

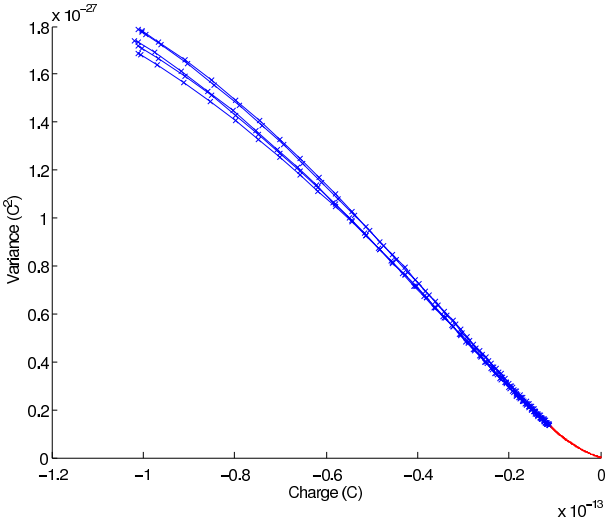

Figure 8.3: *Examples of charge-variance curves. Note the curve fitting was only applied to the blue parts of the curves. Confidence intervals for samples not shown to avoid clutter. 5000 spike samples used per curve.*

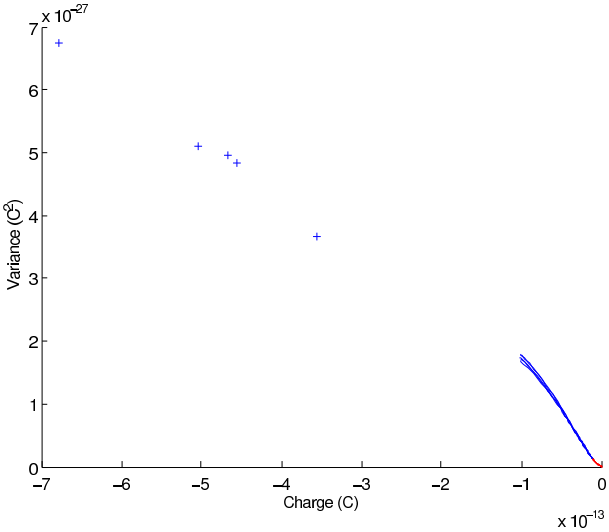

Figure 8.4: Finding the peaks of the 5 curves plotted in figure 8.3.

and so:

$$N = \frac{Q_T}{i_0 \frac{2a+b-2c}{ab-bc}} \tag{8.4}$$

To find the estimate of N we need the values of a,b, and c. From section 5.2.1, it was stated that: a=4240s^{-1}, b=900s^{-1} and c=3260s^{-1}. We'll assume $i_0 \approx 1.4pA$. Substituting these values in we find that:

$$\frac{2a+b-2c}{ab-bc} = 3.24 \times 10^{-3}$$

so we find that:

$$N = \frac{476 \pm 12 \times 10^{-15}}{1.4 \times 10^{-12} \times 3.24 \times 10^{-3}} \tag{8.5}$$

$$N = 104.8 \pm 2.6 \tag{8.6}$$

This is slightly above the actual number (100). This may be because the shape of the curve is still not correctly parabolic, due to the cable filtering or the assumptions made about the channel kinetics.

8.7 Number of iterations

Although a quantitative assessment hasn't been made, it seems the number of measurements required for the charge and current-based techniques is broadly similar.

Estimating the number of channels requires more samples, especially with low open probabilities, as mentioned before. This is a potential problem for either technique.

8.8 Summary

A good estimate for i_0 is possible, but requires knowledge of the steady-state cable filtering of the dendrite and the kinetics of the channel. It is also altered by the number of channels, and can be affected by uncorrelated noise.

Chapter 9

Conclusion

9.1 The Problem

Over the last couple of decades, synapses have been investigated using current-based noise analysis. This uses the fluctuations in the current flow through the synapse to estimate features of the synapse. The feature most closely considered in this thesis has been the channel conductance, but the number of channels, their open probability and more can be discovered using this technique.

Many synapses are a long distance from the soma, which causes their current to be distorted on its way from the synapse to the soma. This distortion alters the fluctuations needed by the noise-analysis, biasing the results.

9.2 The Solution

This thesis proposes that fluctuations in the total charge that flow through the synapse be analysed, rather than fluctuations in current. The charge will be less affected by the dendrite's cable filtering, and can be recorded in the same way as the current. This will allow distant synapses to be analysed, thus allowing important changes in synaptic behaviour to be understood.

9.3 Results

The thesis began by examining theoretical models of ion channels. By considering the state diagram of a channel, its behaviour can be simulated. Using these models, the expected charge fluctuations can be calculated. This allowed the charge-variance plots to be understood, and key features calculated from them. It was found that the charge-based analysis could replicate the current-based analysis for local synapses. The analysis was applied to distant AMPA synapses, and the discrepancy caused by cable filtering was explained and corrected for.

The technique outlined in the thesis required made many assumptions, but is a useful first step towards applying the charge-based analysis to real experimental data.

9.4 Unsolved Problems

Although the charge-based analysis holds promise, there are many problems still to be resolved, below are a few of them.

Noise Both the charge and current based techniques are susceptible to noise. Microelectrode recordings are inherently noisy. For distant synapses, the noise will be proportionally much greater than for local synapses.

Number of channels To calculate the number of channels, the size of the parabola must be estimated. This is only possible if the mean-variance plot begins to curve, rather than remaining approximately straight. To detect the curvature reduce noise, increase the number of samples and increase the ratio of open channels. Fitting the parabola is a challenge using either technique.

Information requirements The charge-based noise analysis requires the channel's kinetics to be known in advance. Many channel types are now known, but variations, even within a channel type, could distort the results. Similarly, to compensate for cable filtering, the electrotonic distance to the synapse must be known. Techniques exist that potentially could estimate this, but not very reliably.

Model Simplifications The model used in the analysis has been simplified in many ways, for example: The infinite cable assumption, the simplified kinetics (e.g. ignoring inactivated states), the constant transition matrix, an unchanging synapse, etc. These assumptions held for the NeuronC model, but may fail for real experimental results.

Single Synapse In the model, only a single synapse is considered. In a real *in vitro* or *in vivo* experiment, the recording at the soma can expect to detect the firing of many synapses, often simultaneously. How this affects the analysis if these are at different distances, or are of different types has not been considered.

Gradient Estimate The estimate of the gradient was, in the end, possibly over simplified. To apply this to real data, a more complex measure may be needed, that can account for the parabolic curve and the cable-filtering.

9.5 Further Work

There is much work still to do before this technique can be used experimentally. The above list of unsolved problems are clearly potential starting points for future research. Other directions are listed below.

Understanding the cause of the underestimate Why more channels cause the estimate to fall has not yet been investigated, although several possibilities have been listed. A better understanding of how NeuronC models the synapse may help explain this. It could be that numerical-calculation effects are creeping into the analysis, as the model may not be modelling the behaviour accurately enough for the analysis.

Electrotonic distance to synapse Being able to estimate the electrotonic distance to the synapse will allow the correction factor to be applied to the estimates from the analysis. Appendix B briefly looks at the literature and applies some of the published techniques to the NeuronC model.

Channel Types This project has only looked at the AMPA receptor. Other receptors could be analysed in the same way, but each will need a markov model and must be tested analytically.

Real experimental data The next step will be to apply the technique to real experimental data. First for a local synapse, and later for a distant synapse. This will need to be validated by comparison with results from other techniques. For instance, the size of the channels may already be known using patch clamp recordings.

9.6 Summary

This thesis has introduced the charge-based technique for analysing synapses. The technique has been developed and tested on a simulated synapse, and shown to accurately estimate important channel features, even when distorted by cable filtering.

Appendix A

AMPA receptor

The AMPA receptor used by NeuronC is based on Jonas et al's[8, pp 655-656] AMPA receptor. Below is a table recording the transition rates estimated in their paper:

Transition	Rate
f_1	$4.59 \times 10^6 M^{-1} s^{-1}$
r_1	$4.26 \times 10^3 s^{-1}$
f_2	$28.4 \times 10^6 M^{-1} s^{-1}$
r_2	$3.26 \times 10^3 s^{-1}$
f_3	$4.59 \times 10^6 M^{-1} s^{-1}$
r_3	$45.7 s^{-1}$
a	$4.24 \times 10^3 s^{-1}$
b	$900 s^{-1}$
a_1	$2.89 \times 10^3 s^{-1}$
b_1	$39.2 s^{-1}$
a_2	$172 s^{-1}$
b_2	$0.727 s^{-1}$
a_3	$17.7 s^{-1}$
b_3	$4.0 s^{-1}$
a_4	$16.8 s^{-1}$
b_4	$190.4 s^{-1}$

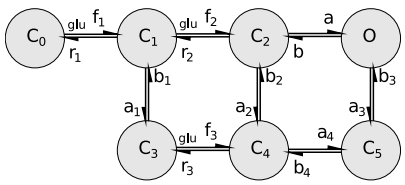

Figure A.1: *The AMPA state model used by the NeuronC modelling software.*

Appendix B

Estimating the Electrotonic distance to the Synapse

B.1 Purpose

As mentioned in section 8.2, the electrotonic distance to the synapse is required to correct for the distortion caused by cable filtering. This length can potentially be found from the shape of the microelectrode recording. This topic is slightly outside the remit of this thesis, but is vital for successfully applying the charge-based noise analysis, and so is briefly covered below.

B.2 A note about Half-Width and Time to Peak

The Half Width is the length of time the voltage is greater than half its peak (figure B.1(a)). The time to peak is more complicated: Deciding when the curve starts is potentially quite arbitrary. Rall[14] suggests plotting a line through the points $\frac{1}{10}$ and $\frac{1}{2}$ of the peak value and finding the intersect point with the x-axis (figure B.1(b)) and using this as the start of the curve. This is the technique used in the following section.

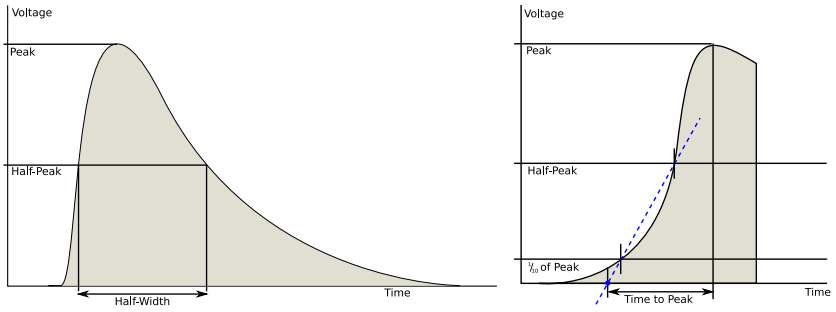

(a) Half Width (b) Time to Peak

Figure B.1: *The half-width and time-to-peak are ways of describing the shape of the curve*

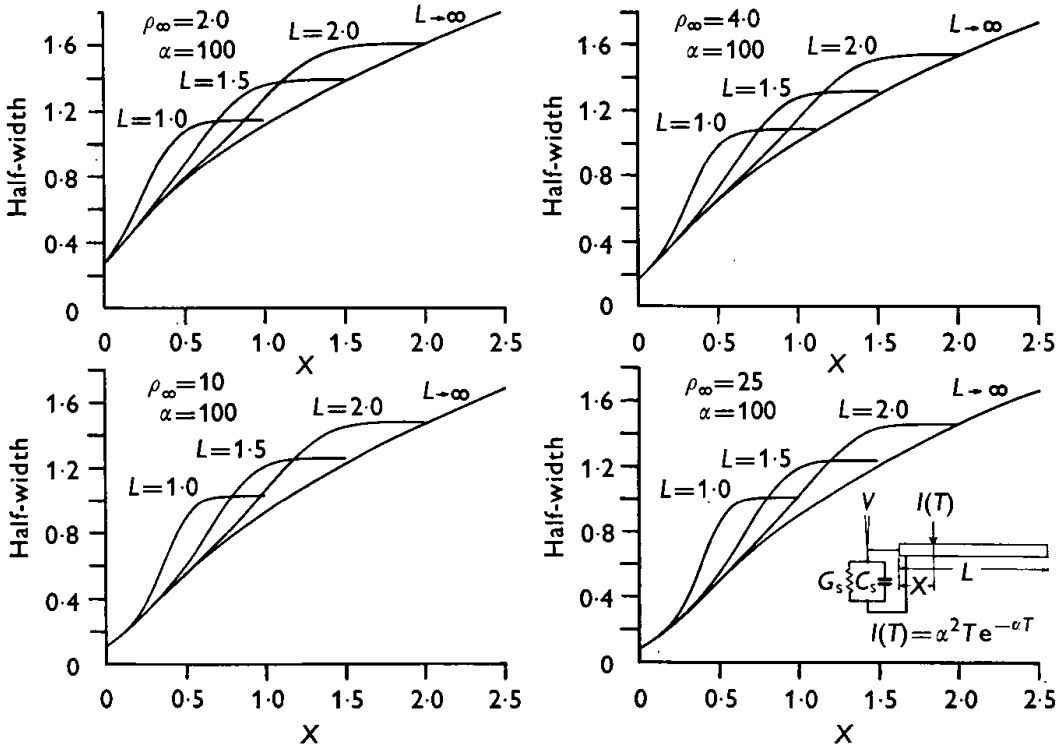

Figure B.2: *These curves indicate the relationship between half-width and distance along the dendritic cable, for values of* ρ_∞ *= 2, 4, 10 and 25, and cable lengths of 1, 1.5 and 2. The assumed current injection time course is* $\alpha^2 T e^{-\alpha T}$*, with* $\alpha = 100$*.* Figure and caption taken from Jack and Redman 1971[7].

B.3 Published Techniques

The shape of the ensemble curve (the mean of the individual spikes) may be able to provide an estimate of the electrotonic length.

Most of the literature that estimates a dendrite's electrotonic length begins by recording the voltage response to a current pulse applied at the *soma*. This allows the ratio of the soma/dendrite conductance, ρ_∞ to be estimated.

Figure 10 of Jack and Redman's 1971 paper (figure B.2)[7] illustrates the relationship between various features of the cell, and the electrotonic distance to the synapse. The variables they use to describe the cell are:

- the electrotonic length of the dendrite, L
- the electrotonic distance between the synapse and soma, X
- the ratio of conductance between a theoretically infinite dendrite and soma, ρ_∞
- the time constant describing the current injection, α

Rall in 1967[14] used a numerical compartmental model to estimate various features of the

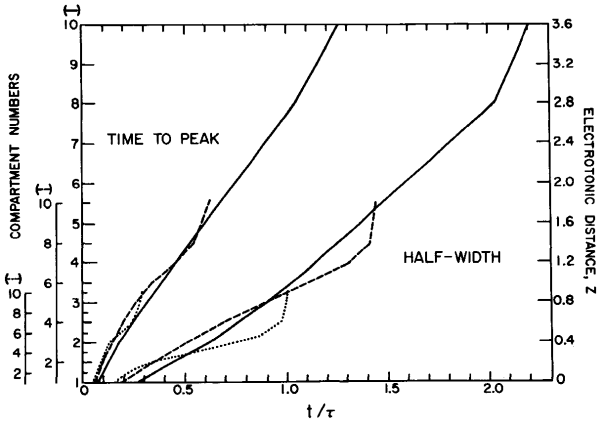

Figure B.3: *Effect of dendritic length upon EPSP shape index values. Three cases, ΔZ = 0.1, 0.2, and 0.4 per dendritic compartment, are shown. The three sets of compartment numbers, shown at left, are spaced to fit a common ordinate scale, expressed as electrotonic distance, Z, shown at right. For each input location (as ordinate), both the time-to-peak and the half-width values were plotted (as abscissa).* Figure and caption taken from Rall 1967[14]. *Solid line ΔZ = 0.4, Dashed line ΔZ = 0.2, and Dotted line ΔZ = 0.1.*

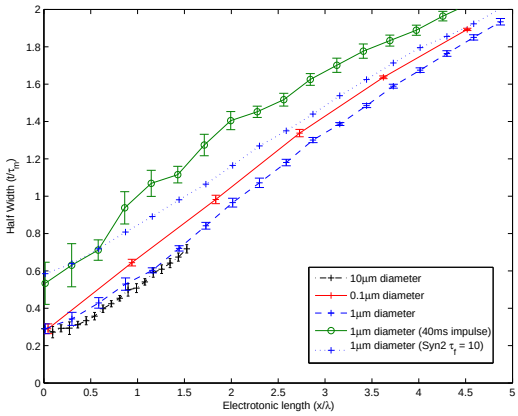

Figure B.4: *Halfwidth vs Electrotonic length for different diameter dendrites*

pulse. Figure B.3 illustrates his results. Notice the gradient, position and shape are very similar to the results in Jack and Redman's 1971 paper.

B.4 NeuronC Results

The electrotonic distance to the synapse is the variable in the following graphs. The voltage injection in the model is a square impulse, on the *presynaptic* side. This is converted into a response (figure B.5) on the post synaptic side. It is unclear how this relates to the time constant α, used in Jack and Redman's paper.

Note that ρ_∞ has yet to be calculated, but its meaning is unclear in this model. Adding or removing the soma has almost no effect on the shape of the response.

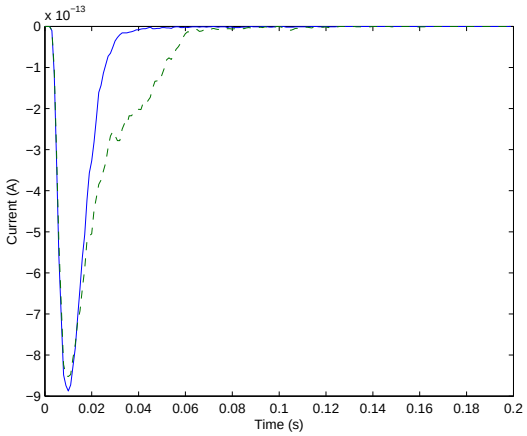

Figure B.5: *Ensemble mean impulse responses (solid blue 1ms pulse, dashed green 4ms pulse).*

Figure B.4 attempts to duplicate the results in figure B.2. Changing the diameter of the dendrite was aimed at altering the value of ρ_∞. It was assumed that the dendrite was long enough that L would be approximately ∞, however if this assumption was false, changing the diameter would also alter L.

Three orders of magnitude of diameter were tried $0.1\mu m$, $1\mu m$ and $10\mu m$. As figure B.4 shows, this has little effect on the gradient of the curve (or its location).

Changing the length of the impulse from 10ms to 40ms appears to have the same effect at all distances, making the curve wider (as might be expected), but only by about $0.2\tau_m$ which is about 8ms (not 4 times as wide, as might be expected). The width remains narrow probably because of channels entering the deactivated state.

B.5 Comparison with published results

The curve in the results from the NeuronC model (figure B.4) is not as steep as the curves in Jack and Redman's graph (figure B.2), or the curve in Rall's (figure B.3). The responses weren't as wide in the NeuronC model as they were in the models used in the papers. This may be because not as much cable filtering occurred, for some reason, or because the impulse was a different shape.

To test this, the Syn2 receptor type was used instead, with $\tau_f = 10ms$, matching the value of $\alpha = 100$. The dot-dashed line in the graph illustrates this. Oddly the gradient of this line is even less than before. This does confirm that the shape of the input is important, and further investigation may show the gradient found in the cited papers. For example using the input $\alpha^2 T e^{-\alpha T}$, as was used in Jack and Redman may generate the expected curve.

Figure B.6 shows both the half-width and the time-to-peak of the NeuronC model attempting to duplicate the Rall results (figure B.3). But both curves (as stated earlier) underestimate

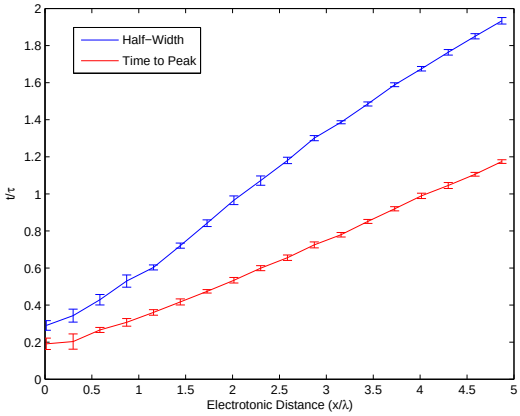

Figure B.6: *How the halfwidth and time to peak vary with electrotonic length*

the half-width and time-to-peak.

B.6 Summary

Alternative stimulation methods (such as a microelectrode providing a controlled current) may allow a closer match to the published results. Also other effects, such as the end-effect may need to be taken into account.

These investigations are beyond the scope of this project, but would potentially allow the distortion in both the charge-based and current-based techniques to be compensated for.

Appendix C

Implementation

C.1 Matlab Simulation

The project's development began with the simulation of the channels in Matlab. `states2.m` is the matlab script that is used to generate the state occupancy data. Program listing 1 shows the two steps used in the central loop of the script to generate the new states. This used the two support scripts; `calcprobs.m` in listing 2 and `genstate.m` in listing 3.

Listing 1 The central loop within the `states2.m` state generator.

```
for (i = 1:size(state,2))
  probs = calcprobs(state(:,i),m,step);
  state = genstate(probs);
end
```

Listing 2 `calcprobs.m` calculates the probability of being in the different states in the next iteration.

```
function probs = calcprobs(oldstate, M, step)
  M = M + eye(size(oldstate,1));
  M = (M^step);
  probs = M*oldstate;
```

The array of states is then analysed by other scripts, such as `getfit.m` to find the parameters of the parabola. A matlab cable model, `cable_filter_analysis.m` was written that simulated the effect of cable filtering on the current, using a simple compartment model.

C.2 NeuronC

The main part of the project used the NeuronC model. This relied on matlab scripts to run and analyse the model and generate the mean-variance plot. The model itself is defined by the

Listing 3 genstate.m selects a state based on the probabilities in the probability vector probs.

```
function newstate = genstate(probs)
  number = rand;
  height = size(probs,1);
  for i = 1:height
    if (number<probs(i))
      newstate = zeros(height,1);
      newstate(i) = 1;
      break;
    else
      number = number - probs(i);
    end
  end
```

test1.n script. The neuronC.m matlab script called and processed the results of the NeuronC model. Other scripts were used to process different aspects of the neuronC model. For instance, NeuronC_record generated the average ensemble.

Listing 4 Section of the neuronC.m script. The program calls the NeuronC script, and processes its results.

```
command = sprintf('../nc/src/nc -r %i -s channels %i ../nc/proj/test1.n
                       | grep -v "^#" > /tmp/temp.dat',seed,channels);
system(command);
load /tmp/temp.dat;
...
for i=1:size(data,1)-1
 chargedata = [chargedata; trapz(data(i:end,:)).*stepsize];
end
data = chargedata;
fit = getfit(data)
```

In section 5.2.1 the model had to be run with different transition rates. This meant changing constants defined in chanampa.cc. To do this a comment was added to the lines that needed changing, and a regular expression applied to update the line with a new rate. NeuronC was then rebuilt using make, and the simulation repeated.

C.3 Distributed Operation

To calculate the confidence intervals of the curve's initial gradient, at least 25 curves had to be plotted and their initial gradient calculated. Much of the research revolved around adjusting a

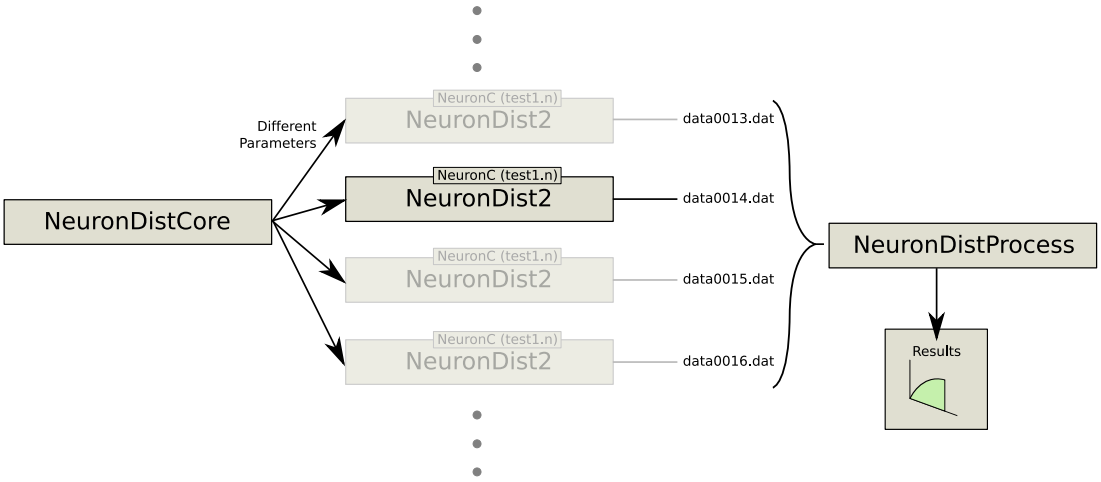

Figure C.1: *Distributive processing. The NeuronDist2 script is run on many computers. On each it calls the NeuronC model. After processing the results locally, a data file is saved, and the script exits.*

parameter and seeing the effect on the initial gradient. This meant finding the initial gradient for several different parameter values. The NeuronC model could take up to 10 minutes, if modelling a long dendrite. Generating enough data for one graph could take up to 2 days of processing time. To avoid this delay, the simulation was distributed over approximately 100 computers.

A list of hosts that are probably dice machines was found using `nmap -sT 129.215.58.* -p 22`. The list was processed and then used by the matlab script `NeuronDistCore.m` to distribute jobs. This script called `ssh` and ran, using matlab, an instance of `NeuronDist2.m`, with a set of parameters passed to it. This called the NeuronC model, and processed the results, before saving the gradient in a unique file, such as `project/rawdata/data0042.dat`. These data files are later read by the `NeuronDistProcess.m` script and collated into a graph.

C.4 Summary

The implementation was not central to the projects aims, and it should be possible to reproduce the same results with a new implementation. The processing was quite straightforward and any important points have been mentioned in the thesis. The full source code is available on request.

Listing 5 Section of the neuronC model code. The presynaptic 'neuron' is made of one compartment labelled `pre`. The post synaptic compartment is number 1, and a series of compartments from 1 to `no_of_cable_segs` represent the dendrite to the Soma. The extra cable is connected to compartment 1 - to represent the rest of the dendrite.

```
  at pre sphere dia 1;

/*Make Synapse */
  conn pre to 1 synapse linear 5 maxcond=channels*unit_cond
  resp ampa
  chnoise=1  N=channels
  nfilt3 0 timec3=0.5 /* no after binding filtering */
  vrev=0 nfilt1 1 timec1 1
  ename thesynapse;

  for (i = 1;i<no_of_cable_segs;i++)
  {
    conn i to i+1 cable length seg_len dia diam; /* Make cable */
  };

  /*Extra segments*/
  for (i = no_of_cable_segs+1;i<no_of_cable_segs+extra_cable_segs;i++)
  {
    conn i to i+1 cable length extra_seg_len dia diam;
  };
  conn 1 to no_of_cable_segs+1 cable length extra_seg_len dia 1; /* Connect extra cable to rest */

  at no_of_cable_segs sphere dia 100; /*add Soma*/

  stim node no_of_cable_segs vclamp -0.07 start 0 dur 5000;
  for (j = 0;j<50000;j++)
  {
    stim node pre vclamp -.025 start j*0.2 dur .01; /* voltage clamp */
  };
  plot I[no_of_cable_segs];
```

Appendix D

Initial Gradient Proof for O $\longrightarrow$ O $\longrightarrow$ C kinetics

D.1 The Initial Gradient Equation

The charge and variance for the O $\rightarrow_a$ O $\rightarrow_b$ C kinetics, as described in section 3.2.5 can be found using the analytical method laid out in section 3.1. This gives:

$$\langle Q \rangle(t) = -\frac{b^2 e^{-at} - a^2 e^{-bt}}{a^2 b - a b^2} \tag{D.1}$$

$$\sigma_Q^2 = -\frac{(b^2 e^{-at} - a^2 e^{bt})^2}{(a^2 b - a b^2)^2} - \frac{2b^3 e^{-at} - 2a^3 e^{-bt}}{a^3 b^2 - a^2 b^3} \tag{D.2}$$

The initial gradient of the variance-charge curve is equal to the derivative of the variance over the derivative of the charge, with respect to time, as time approaches ∞. L'Hôptial's rule means this can be written as the ratio of the variance and the charge.

$$\left.\frac{d\sigma_Q^2}{d\langle Q \rangle}\right|_{t\to\infty} = \frac{\sigma_Q^2(t \to \infty)}{Q(t \to \infty)} \tag{D.3}$$

This ratio is equal to:

$$\left.\frac{d\sigma_Q^2}{d\langle Q \rangle}\right|_{t\to\infty} = \left.\frac{(a-b)(\frac{2ab^3 e^{-at} - 2a^3 b e^{-bt}}{a-b} + \frac{2abe^{-2(a+b)t}(ae^{at} - be^{bt})(a^2 e^{at} - b^2 e^{bt})}{(a-b)^2})}{a^2 b^2 (be^{-at} - a^{-bt})}\right|_{t\to\infty} \tag{D.4}$$

It is assumed that both a and b are greater than zero. If they were less, then the transition matrix would be for a different kinetics. For example if b were negative, the channels would never be able to reach the closed state.

Note that the equation is symmetrical, in that a and b could be swapped without altering the result. If a and b were swapped, each bracketed term would give either the same value, or its negative. It can be seen by inspection that these negatives will cancel out. For example $(ae^{at} - be^{bt})$ would swap sign if a and b were swapped, but so would $(a^2 e^{at} - b^2 e^{bt})$, so the overall sign would remain the same.

D.2 The First Two Terms

Starting with the first two terms from equation D.4:

$$\frac{(a-b)\frac{2ab^3e^{-at}-2a^3be^{-bt}}{a-b}}{a^2b^2(be^{-at}-a^{-bt})} \tag{D.5}$$

Simplify and divide through by e^{-at}:

$$\frac{1}{a^2b^2}\left(\frac{2ab^3}{b-ae^{a-b}}-\frac{2a^3b}{a-be^{t(b-a)}}\right) \tag{D.6}$$

Because a and b are symmetric in the original equation, if we assume that $a \neq b$ then we can arbitrarily state that $a > b$ in the following proof, and then reverse the result for the case where $b > a$.

By defining $a > b$, it can be seen that as $t \to \infty$ the exponential term, $e^{t(b-a)} \to 0$, because $b-a < 0$. This exponential term can be removed, leaving:

$$\frac{1}{a^2b^2}\left(\frac{2ab^3}{b-ae^{a-b}}-\frac{2a^3b}{a}\right) \tag{D.7}$$

As $t \to \infty$, the ae^{a-b} term will approach ∞, which will cause the left hand term to tend to zero. So, as $t \to \infty$, the statement will approach:

$$\frac{1}{a^2b^2}\left(\frac{2a^3b}{a}\right)=\frac{2}{b} \tag{D.8}$$

D.3 The Remaining Terms Approach Zero

The rest of the equation can be multipled out into four terms:

$$\frac{2a^3e^{-2bt}-2ab^2e^{-(a+b)t}-2a^2be^{-(a+b)t}+2b^3e^{-2at}}{(a-b)ab(be^{-at}-ae^{-bt})} \tag{D.9}$$

Consider each separately, it can be seen they all tend to zero, as $t \to \infty$:

The first term can be written

$$\frac{2a^2}{(a-b)b(be^{(2b-a)t}-ae^{bt})} \tag{D.10}$$

It has been assumed that both a and b are greater than zero. This means the second exponential will definitely approach ∞, causing the term to approach zero, as $t \to \infty$.

The second and third terms can be combined:

$$\left(\frac{2ab^2+2a^2b}{(a-b)ab}\right)\left(\frac{e^{-(a+b)t}}{be^{-at}-ae^{-bt}}\right) \tag{D.11}$$

Again, divide through by the numerator's exponential. The denominator of the second half of the equation becomes:

$$be^{bt}-ae^{at} \tag{D.12}$$

Using the assumption that both a and b are greater than zero and are not equal, the expression will tend to ∞ as $t \to \infty$, causing the whole term to approach zero.

The last term, can be treated similarly, and is found to have in the denominator, the term:

$$be^{at} - ae^{(2a-b)t} \tag{D.13}$$

Of which the first exponential, e^{at} will approach ∞, causing the final term to tend to zero, as $t \to \infty$.

D.4 Summary

The only term that doesn't tend to zero, as $t \to \infty$, is the one that tends to $\frac{2}{b}$. Note that b was defined to be less than a. The equation treats both a and b identically, so the result can be summarised as follows:

$$\left.\frac{d\sigma_Q^2(t)}{d\langle Q\rangle(t)}\right|_{t\to\infty} = \frac{2}{min(a,b)} \tag{D.14}$$

Intuitively, the time it takes for a channel to get into the closed state depends on both a and b. However, in the limit, for large t, the time it takes to close depends on the slowest rate alone.

Bibliography

[1] D. J. Aidley and P. R. Stanfield. *Ion Channels*. Cambridge University Press, first edition edition, 1996.

[2] A. Destexhe, Z. F. Mainen, and T. J. Sejnowski. *Kinetic Models of Synaptic Transmission*. MIT Press, 2nd edition edition, 1998.

[3] L. Galvani and M. G. Foley. *Commentary on the effects of electricity on muscular motion*. Burndy Library, 1953. Originally published 1793.

[4] O. P. Hamill, A. Marty, E. Neher, B. Sakmann, and F. J. Sigworth. Improved patch-clamp techniques for high-resolution current recording from cells and cell-free membrane patches. *Pflügers Archiv European Journal of Physiology*, 391(2):85–100, August 1981.

[5] A. L. Hodgkin and A. F. Huxley. A quantitative description of membrane current and its application to conduction and excitation in nerve. *The Journal of Physiology*, 117:500–544, 1952.

[6] R. Iansek and S. J. Redman. An analysis of the cable properties of spinal motoneurones using a brief intracellular current pulse. *The Journal of Physiology*, 234:613–636, 1973.

[7] J. J. B. Jack and S. J. Redman. An electrical description of the motoneurone, and its application to the analysis of synaptic potentials. *The Journal of Physiology*, 215:321–352, 1971.

[8] P. Jonas, G. Major, and B. Sakmann. Quantal components of unitary EPSCs at the mossy fibre synapse on ca3 pyramidal cells of rat hippocampus. *The Journal of Physiology*, 472:615–663, 1993.

[9] D. Y. Kim, S. H. Kim, H. B. Choi, C.-k. Min, and B. J. Gwag. High abundance of GluR1 MRNA and reduced q/r editing of GluR2 MRNA in individual NADPH-Diaphorase neurons. *Molecular and Cellular Neuroscience*, 17:1025–1033, 2001.

[10] M. Megías, Z. Emri, T. Freund, and A. Gulyás. Total number and distribution of inhibitory and excitatory synapses on hippocampal ca1 pyramidal cells. *Neuroscience*, 102(3):527–540, February 2001.

[11] T. Narahashi, J. W. Moore, and W. R. Scott. Tetrodotoxin blockage of sodium conductance increase in lobster giant axons. *The Journal of General Physiology*, 47:965–974, 1964.

[12] K. M. Partin, M. W. Fleck, and M. L. Mayer. AMPA receptor flip/flop mutants affecting deactivation, desensitization, and modulation by cyclothiazide, aniracetam, and thiocyanate. *The Journal of Neuroscience*, 16(21):6634–6647, November 1996.

[13] J. Pearce. Sir charles scott sherrington (1857–1952) and the synapse. *Journal of Neurology, Neurosurgery & Psychiatry*, 75(4):544, April 2004.

[14] W. Rall. Distinguishing theoretical synaptic potentials computed for different soma-dendritic distributions of synaptic input. *Journal of Neurophysiology*, 30:1138–1168, 1967.

[15] M. Raman and L. O. Trussell. The mechanism of alpha-amino-3-hydroxy-5-methyl-4-isoxazolepropionate receptor desensitization after removal of glutamate. *Biophysical Journal*, 68:137–146, 1995.

[16] S. Redman and B. Walmsley. The time course of synaptic potentials evoked in cat spinal motoneurones at identified group ia synapses. *The Journal of Physiology*, 343:117–133, 1983.

[17] H. P. C. Robinson, Y. Sahara, and N. Kawai. Nonstationary fluctuation analysis and direct resolution of single channel currents at postsynaptic sites. *Biophysical Journal*, 59:295–304, February 1991.

[18] F. J. Sigworth. The variance of sodium current fluctuations at the node of ranvier. *The Journal of Physiology*, 307:97–129, 1980.

[19] R. G. Smith. NeuronC: a computational language for investigating functional architecture of neural circuits. *Journal of Neuroscience Methods*, 43(2-3):83–108, July 1992.

[20] G. Squires. *Practical Physics*. Cambridge University Press, 3rd edition, 1985.

[21] C. F. Stevens. Inferences about membrane properties from electrical noise measurements. *Biophysical Journal*, 12:1028–1047, 1972.

[22] G. J. Stuart, H. U. Dodt, and B. Sakmann. Patch-clamp recordings from the soma and dendrites of neurons in brain slices using infrared video microscopy. *Pflügers Archiv European Journal of Physiology*, 423(5-6):511–518, June 1993.

[23] R. J. van den Berg, J. de Goede, and A. A. Verveen. Conductance fluctuations in ranvier nodes. *Pflügers Archiv European Journal of Physiology*, 360:17–23, 1975.

[24] P. Wildman. Estimating a population standard deviation or variance. *http://wind.cc.whecn.edu/~pwildman/statnew/estimating_a_population_standard_devation_or_variance.htm*, accessed July, 2008.